

*Electronic Supplementary Information*

**Discrepancy between thermodynamic and kinetic stabilities of the tert-butanol hydrates and its implication on obtaining pharmaceutical powders by freeze-drying**

Andrey G. Ogienko<sup>a,b,\*</sup>, Andrey S. Stoporev<sup>a,b,c</sup>, Anna A. Ogienko<sup>a,d</sup>, Maxim S. Mel'gunov<sup>b,e</sup>, Tatyana P. Adamova<sup>a</sup>, Alexander S. Yunoshev<sup>b,f</sup>, Andrey Yu. Manakov<sup>a,b</sup>, Elena V. Boldyreva<sup>b,e,\*</sup>

<sup>a</sup> Nikolaev Institute of Inorganic Chemistry SB RAS, 630090, Novosibirsk, Russia.

<sup>b</sup> Department of Natural Sciences, Novosibirsk State University, 630090, Novosibirsk, Russia

<sup>c</sup> Department of Physical and Colloid Chemistry, Gubkin University, 119991, Moscow, Russia

<sup>d</sup> Institute of Molecular and Cellular Biology SB RAS, 630090, Novosibirsk, Russia

<sup>e</sup> Boreskov Institute of Catalysis SB RAS, 630090, Novosibirsk, Russia

<sup>f</sup> Lavrentiev Institute of Hydrodynamics SB RAS, 630090, Novosibirsk, Russia

\* Corresponding authors:

Andrey G. Ogienko

Nikolaev Institute of Inorganic Chemistry SB RAS, Lavrentiev ave. 3, Novosibirsk 630090, Russia.

Novosibirsk State University, ul. Pirogova 2, Novosibirsk 630090, Russia

Tel: +7 (383)3165346 Fax: +7 (383) 3309489 E-mail: [ogienko@niic.nsc.ru](mailto:ogienko@niic.nsc.ru)

Elena V. Boldyreva

Boreskov Institute of Catalysis SB RAS, Lavrentiev ave 5, Novosibirsk 630090, Russia

Novosibirsk State University, ul. Pirogova 2, Novosibirsk 630090, Russia

Tel: +7 (383) 3634272 Fax: +7 (383) 3309489 E-mail: [eboldyreva@catalysis.ru](mailto:eboldyreva@catalysis.ru)

## Table of contents

### ABBREVIATIONS

**Figure S1.** Several variants of the TBA–water system phase diagram based on the data of Rosso and Carbonnel, Ott *et al.*, Mootz and Staben (*a*)<sup>1-3</sup>, Rosso and Carbonnel, Mootz and Staben, Woznyj and Lüdemann (*b*)<sup>1,2,4</sup>, Kasraian and DeLuca (*c*)<sup>5</sup>. “Extended” variant based on data of Vessot and Andrieu, Kasraian and DeLuca, Dobrzycki<sup>5-7</sup> and our experimental (PXRD+TA) data (*d*) and a variant which can be realized at a higher pressure (*e*). Temperature of metastable *Ih*+H1 eutectic melting on (*b*): (1) – Rosso and Carbonnel,<sup>1</sup> Ott *et al.*<sup>2</sup> (2) – Woznyj and Lüdemann<sup>4</sup> (dashed lines).

### EXPERIMENTAL DETAILS

1. Low-temperature PXRD (powder X-ray diffraction) experiments

**Figure S2.** Samples (№№ 1-7) for low-temperature PXRD on water–TBA composition line.

**Figure S3.** Estimated cooling rates corresponding to different freezing protocols. *a* – vials in an air thermostat (protocol Ia), -20°C; *b* – vial in a cryothermostat at -50°C (protocol IIa); *c* – vials in a vessel with liquid nitrogen (protocol IIIa\_vial).

2. DSC experiments

3. TA experiments

4. Measurements of sublimation rate

5. Determination of sublimation behavior of TBA hydrates

6. Scanning electron microscopy (SEM)

### RESULTS

**Extended version of Table 2 from the main text.** Results of the low-temperature PXRD experiments aimed at identifying the phases formed on freezing and subsequent annealing in the TBA–water system. Annealing defines heating the sample from the freezing temperature to -20°C and keeping at these conditions up to 3 months. The main phase of the sample is indicated first. The admixture phases (giving a few weak reflections on PXRD patterns) are shown in brackets.

**Figure S4.** PXRD patterns of frozen TBA–water solutions recorded at -100°C (*a* – protocol Ia, *b* – protocol IIa, *c* – protocol IIIa). The positions of reflections of the TBA hydrates (H1 and H2) and ice *Ih* are shown as ticks at the bottom. The positions of reflections of the H3 TBA hydrate are not shown for clarity. \* – the strongest reflections of the TBA. 1, 2, 3, 4, 5, 6, 7 – correspond to 10, 20, 29.8 (H3), 37 (H2), 55, 70 (H1) and 85 wt % of TBA, respectively. The admixture phases (a few weak reflections on PXRD patterns) are shown in brackets.

**Figure S5.** PXRD patterns of frozen TBA–water solutions (10 wt % of TBA) at different temperatures (*a* – protocol Ia, *b* – protocol IIa, *c* – protocol IIIa). The positions of reflections of the TBA hydrates (H1 and H2) and ice *Ih* are shown as ticks at the bottom. The strongest reflections of the H2 (figure *b*) are pointed by arrows. The admixture phases (a few weak reflections on PXRD patterns) are shown in brackets.

**Figure S6.** PXRD patterns of frozen TBA–water solutions (20 wt % of TBA) at different temperatures (*a* – protocol Ia, *b* – protocol IIa, *c* – protocol IIIa). The positions of reflections of the TBA hydrates (H1, H2, H3) and ice *Ih* are shown as ticks at the bottom. The admixture phases (a few weak reflections on PXRD patterns) are shown in brackets.

**Figure S7.** PXRD patterns of frozen TBA–water solutions (29.8 wt % of TBA, H3 composition) at different temperatures (*a* – protocol Ia, *b* – protocol IIa, *c* – protocol IIIa). The positions of reflections of the TBA hydrates (H1, H2, H3) and ice *Ih* are shown as ticks at the bottom. The strongest reflections of the H2 (figure *b*) and ice *Ih* (figure *c*) phases are pointed by navy arrows. The admixture phases (a few weak reflections on PXRD patterns) are shown in brackets.

**Figure S8.** PXRD patterns of frozen TBA–water solutions (37 wt % of TBA, H2 composition) at different temperatures (*a* – protocol Ia, *b* – protocol IIa, *c* – protocol IIIa). The positions of reflections of the TBA hydrates (H1, H2, H3) and ice *Ih* are shown as ticks at the bottom. The strongest reflections of the unidentified phase (H3) (figure *b*) are pointed by red arrows. The admixture phases (a few weak reflections on PXRD patterns) are shown in brackets.

**Figure S9.** PXRD patterns of frozen TBA–water solutions (55 wt % of TBA) at different temperatures (*a* – protocol Ia, *b* – protocol IIa, *c* – protocol IIIa). The positions of reflections of the TBA hydrates (H1, H2, H3) and ice *Ih* are shown as ticks at the bottom. The strongest reflections of the unidentified phase (H3) (figure *c*) are pointed by red arrows. The appearance of H2 reflections pointed by navy arrows. The admixture phases (a few weak reflections on PXRD patterns) are shown in brackets.

**Figure S10.** PXRD patterns of frozen TBA–water solutions (70 wt % of TBA, H1 hydrate composition) at different temperatures (*a* – protocol Ia, *b* – protocol IIa, *c* – protocol IIIa). The positions of reflections of the H1 and TBA are shown as ticks at the bottom. The strongest reflections of the TBA (figures *a* and *c*) are pointed by navy arrows. The admixture phases (a few weak reflections on PXRD patterns) are shown in brackets.

**Figure S11.** PXRD patterns of frozen TBA–water solutions (85 wt % of TBA) at different temperatures (*a* – protocol Ia, *b* – protocol IIa, *c* – protocol IIIa). The positions of reflections of the H1 and TBA are shown as ticks at the bottom.

**Figure S12.** Typical experimental curves obtained in TA experiments (cooling and subsequent heating). Cooling rate of  $\sim 1^\circ\text{C}/\text{min}$  (similar to protocol Ia). *a* (magenta line) – 10 wt % of TBA, *b* (red line) – 29.8 wt % of TBA (H3 composition).

**Figure S13.** Comparison of thermal effects, obtained in TA experiments (on heating) for samples of solutions frozen according to protocol Ia (*a* (magenta line) – 10 wt % of TBA; *b* (red line) – 29.8 wt % of TBA) and protocol IIIa (“cold loading”, *c* (navy line) – 29.8 wt % of TBA).

The TA curve measured on heating the solution of H3 hydrate composition (29.8 wt % of TBA) frozen according to protocol IIIa (*c*) shows two thermal effects at  $-8.2$  and  $-5.7^\circ\text{C}$  that agrees well with data of (Rosso and Carbonnel, 1968; Ott *et al.*, 1979; Mootz and Staben, 1993)<sup>1-3</sup> and corresponds to the “H2+*Ih*” eutectic melting ( $Ih + H2 = l$ ) and to the incongruent melting of H2 hydrate ( $H2 = H1 + l$ ). On TA curves measured on

heating the solutions frozen according to protocol Ia (*a*, *b*) show thermal effect at -9.3°C that corresponds to the “H1+I<sub>h</sub>” metastable eutectic melting ( $I_h + H1 = I$ ).

**Figure S14.** PXRD patterns of frozen and subsequently annealed TBA – water solutions recorded at -100°C (*a* – protocol Ib, *b* – protocol IIb, *c* – protocol IIIb). The positions of reflections of the TBA hydrates (H1 and H2) and ice I<sub>h</sub> are shown as ticks at the bottom. \* - the strongest reflections of the TBA. 1, 2, 3, 4, 5, 6, 7 – correspond to 10, 20, 29.8 (H3), 37 (H2), 55, 70 (H1) and 85 wt % of TBA, respectively. The admixture phases (a few weak reflections on PXRD patterns) are shown in brackets.

**Figure S15.** PXRD patterns of frozen and subsequently annealed TBA–water solutions (10 wt % of TBA) at different temperatures (*a* – protocol Ib, *b* – protocol IIb, *c* – protocol IIIb). The positions of reflections of the H2 and ice I<sub>h</sub> are shown as ticks at the bottom.

**Figure S16.** PXRD patterns of frozen and subsequently annealed TBA–water solutions (20 wt % of TBA) at different temperatures (*a* – protocol Ib, *b* – protocol IIb, *c* – protocol IIIb). The positions of reflections of the H2 and ice I<sub>h</sub> are shown as ticks at the bottom.

**Figure S17.** PXRD patterns of frozen and subsequently annealed TBA–water solutions (29.8 wt % of TBA, H3 composition) at different temperatures (*a* – protocol Ib, *b* – protocol IIb, *c* – protocol IIIb). The positions of reflections of the TBA hydrates (H1, H2) and ice I<sub>h</sub> are shown as ticks at the bottom.

**Figure S18.** PXRD patterns of frozen and subsequently annealed TBA–water solutions (37 wt % of TBA, H2 composition) at different temperatures (*a* – protocol Ib, *b* – protocol IIb, *c* – protocol IIIb). The positions of reflections of the TBA hydrates (H1, H2) and ice I<sub>h</sub> are shown as ticks at the bottom. The admixture phases (a few weak reflections on PXRD patterns) are shown in brackets.

**Figure S19.** PXRD patterns of frozen and subsequently annealed (*a* – protocol Ib, *b* – protocol IIb, *c* – protocol IIIb) TBA–water solutions (55 wt % of TBA) at different temperatures. The positions of reflections of the TBA hydrates (H1, H2) and ice I<sub>h</sub> are shown as ticks at the bottom. The admixture phases (a few weak reflections on PXRD patterns) are shown in brackets.

**Figure S20.** PXRD patterns of frozen and subsequently annealed TBA–water solutions (70 wt % of TBA, H1 composition) at different temperatures (*a* – protocol Ib, *b* – protocol IIb, *c* – protocol IIIb). The positions of reflections of the TBA hydrates (H1, H2) and ice I<sub>h</sub> are shown as ticks at the bottom. The admixture phases (a few weak reflections on PXRD patterns) are shown in brackets.

**Figure S21.** Powder diffraction patterns of frozen and subsequently annealed (*a* – protocol Ib, *b* – protocol IIb, *c* – protocol IIIb) TBA–water solutions (85 wt % of TBA) at different temperatures. The positions of reflections of the H1 and TBA are shown as ticks at the bottom.

**Figure S22.** Comparison of PXRD patterns of frozen (*a* – protocol Ia) and subsequently annealed (*b* – protocol Ib) TBA–water solutions recorded at -100°C. The positions of reflections of the TBA hydrates (H1 and H2) and ice I<sub>h</sub> are shown as ticks at the bottom. The positions of reflections of the H3 are not shown for clarity. \* – the strongest reflections of the TBA. 1, 2, 3, 4, 5, 6, 7 – correspond to 10, 20, 29.8 (H3), 37 (H2), 55, 70 (H1) and 85 wt % of TBA, respectively. The admixture phases (a few weak reflections on PXRD patterns) are shown in brackets.

**Figure S23.** Comparison of PXRD patterns of frozen (*a* – protocol II*a*) and subsequently annealed (*b* – protocol II*b*) TBA–water solutions recorded at -100°C. The positions of reflections of the TBA hydrates (H1 and H2) and ice *I<sub>h</sub>* are shown as ticks at the bottom. The positions of reflections of the H3 are not shown for clarity. \* – the strongest reflections of the TBA. 1, 2, 3, 4, 5, 6, 7 correspond to 10, 20, 29.8 (H3), 37 (H2), 55, 70 (H1) and 85 wt % of TBA, respectively. The admixture phases (a few weak reflections on PXRD patterns) are shown in brackets.

**Figure S24.** Comparison of PXRD patterns of frozen (*a* – protocol III*a*) and subsequently annealed (*b* – protocol III*b*) TBA–water solutions recorded at -100°C. The positions of reflections of the TBA hydrates (H1 and H2) and ice *I<sub>h</sub>* are shown as ticks at the bottom. The positions of reflections of the H3 are not shown for clarity. \* – the strongest reflections of the TBA. 1, 2, 3, 4, 5, 6, 7 – correspond to 10, 20, 29.8 (H3), 37 (H2), 55, 70 (H1) and 85 wt % of TBA, respectively. The admixture phases (a few weak reflections on PXRD patterns) are shown in brackets.

**Figure S25.** Comparison of PXRD patterns of frozen (*a* – protocol I*a*) and subsequently annealed (*b*, *c*, *d* – protocol I*b*) TBA–water solutions (29.8 wt % of TBA, H3 composition) at different duration of annealing stage (general view) recorded at -100°C. *b* – 12 hours, *c* – 1 month, *d* – 3 months. The admixture phases (a few weak reflections on PXRD patterns) are shown in brackets.

**Figure S26.** Comparison of PXRD patterns of frozen (*a* – protocol I*a*) and subsequently annealed (*b*, *c*, *d* – protocol I*b*) TBA–water solutions (29.8 wt % of TBA, H3 composition) at different duration of annealing stage recorded at -100°C (enlarged view). *b* – 12 hours, *c* – 1 month, *d* – 3 months. The appearance of reflections of the H2 is shown by navy arrows on *b*. The admixture phases (a few weak reflections on PXRD patterns) are shown in brackets.

**Table S1.** Phases formed from the solutions with the TBA content corresponding to H3 composition (29.8 wt % of TBA) and calculated weight fraction of TBA hydrates and ice *I<sub>h</sub>* depending on freezing protocol.

**Figure S27.** Weight loss vs. time for 15 ml glass tubing vials filled with 2.000±0.005 g of a TBA–water solution (29.8 wt % of TBA, H3 composition). Shelf temperature -10°C, chamber pressure 100 mTorr. *a* – freezing protocol I*a*, solid phases at the beginning of experiment: H1+*I<sub>h</sub>*; *b* – freezing protocol III*b*\_vial, solid phases at the beginning of experiment: H2+*I<sub>h</sub>*; *c* – freezing protocol III*a*\_vial, solid phase at the beginning of experiment: H3.

**Figure S28.** Results of an experiment aimed to determine the sublimation behavior of TBA hydrates in 15 ml glass tubing vials filled with 2.000±0.005 g of TBA–water solution (29.8 wt % of TBA, H3 composition). Shelf temperature -10°C, chamber pressure 100 mTorr. Comparison of PXRD patterns of the samples (*a*: protocol I*a*; *b*: protocol III*a*\_vial; *c*: protocol III*b*\_vial) at different stage of freeze-drying recorded at -100°C (1: starting samples (before placed on drying shelf); 2 – after 50 % weight loss). The admixture phases (a few weak reflections on PXRD patterns) are shown in brackets.

**Figure S29.** Results of an experiment aimed to determine the sublimation behavior of TBA hydrates *in situ* in an Anton Paar TTK 450 low-temperature chamber. Comparison of PXRD patterns of samples (29.8 wt % of TBA, H3 composition; *a*: protocol I*a*; *b*: protocol III*a*\_vial; *c*: protocol III*b*\_vial) at different stage of freeze-

drying (1: starting samples at -100°C/ambient pressure; 2 and 3: after 10 and 20 minutes at -10°C/100 mTorr, respectively). The admixture phases (a few weak reflections on PXRD patterns) are shown in brackets.

**Figure S30.** Results of experiment aimed to determine the sublimation behavior of THF hydrate in 15 ml glass tubing vials filled with  $2.000 \pm 0.005$  g of a THF – water solution (19.1 wt % of THF, THF hydrate composition) (a) *in situ* in an Anton Paar TTK 450 low-temperature chamber (b). Comparison of PXRD patterns of samples at different stages of freeze-drying (a: 1: starting samples before being placed on drying shelf; 2 – after 50 % weight loss; b: 1: starting samples at -100°C/ambient pressure; 2: after 20 minutes at -10°C/100 mTorr, respectively). The positions of the reflections of the CS-II THF hydrate and ice *Ih* are shown as ticks at the bottom.

**Table S2.** Sublimation end points for 15 ml glass tubing vials filled with  $2.000 \pm 0.005$  g of TBA-water solutions (29.8 wt %, H3 composition). Shelf temperature -25°C, chamber pressure 100 mTorr (sample temperature lower than -40°C).

**Figure S31.** PXRD patterns (recorded at -100°C) of trehalose solutions in a TBA–water co-solvent system (29.8 wt % of TBA, H3 composition), frozen according to different protocols. a - freezing protocol IIIa; b - freezing protocol IIIb; c - freezing protocol IIa; d - freezing protocol Ia. The positions of reflections of the TBA hydrates (H1, H2, H3) and ice *Ih* are shown as ticks at the bottom.

**Figure S32.** DSC curves of frozen trehalose solutions (5 wt % of trehalose) in water (a) and a TBA–water co-solvent system (29.8 wt % of TBA, H3 composition) (b). The change of the slope of the basal lines is zoomed.

**Figure S33.** PXRD patterns: a - starting trehalose dihydrate; b - trehalose freeze-dried cake, obtained from aqueous solution (5 wt % of trehalose), freezing protocol Ia; c - trehalose freeze-dried cake, obtained from trehalose solution (5 wt % of trehalose) in TBA–water (29.8 wt % of TBA), freezing protocol Ia; d - trehalose freeze-dried cake, obtained from trehalose solution (5 wt % of trehalose) in TBA–water (29.8 wt % of TBA), freezing protocol IIIb\_vial.

**Figure S34.** DSC curves obtained on heating (6 K/min) of trehalose freeze-dried cakes, prepared from trehalose solutions (5 wt % of trehalose) according to different freezing protocols (a - d) and starting trehalose dihydrate (e). a - trehalose freeze-dried cake, obtained from aqueous solution, freezing protocol Ia; b - trehalose freeze-dried cake, obtained from aqueous solution, freezing protocol IIIa; c - trehalose freeze-dried cake, obtained from trehalose solution in TBA – water (29.8 wt % of TBA), freezing protocol Ia; d - trehalose freeze-dried cake, obtained from trehalose solution in TBA–water (29.8 wt % of TBA), freezing protocol IIIa; e - trehalose freeze-dried cake, obtained from aqueous solution.

**Figure S35.** Internal structure of the trehalose freeze-dried cakes, prepared from 5 wt % of trehalose solutions according to different freezing protocols. a – aqueous solution, freezing protocol Ia, solid phase at the beginning of the experiment: *Ih*; b – TBA–water solution (29.8 wt % of TBA), freezing protocol Ia, solid phases at the beginning of experiment: H1+*Ih*; c – TBA–water solution (29.8 wt % of TBA), freezing protocol IIIb\_vial, solid phases at the beginning of experiment: H2+*Ih*.

## REFERENCES

## ABBREVIATIONS

°C Degrees Centigrade

TBA *tert*-butanol

H1 TBA·2H<sub>2</sub>O

H2 TBA·7H<sub>2</sub>O

H3 TBA·10H<sub>2</sub>O

PXRD powder X-ray diffraction

TA thermal analysis

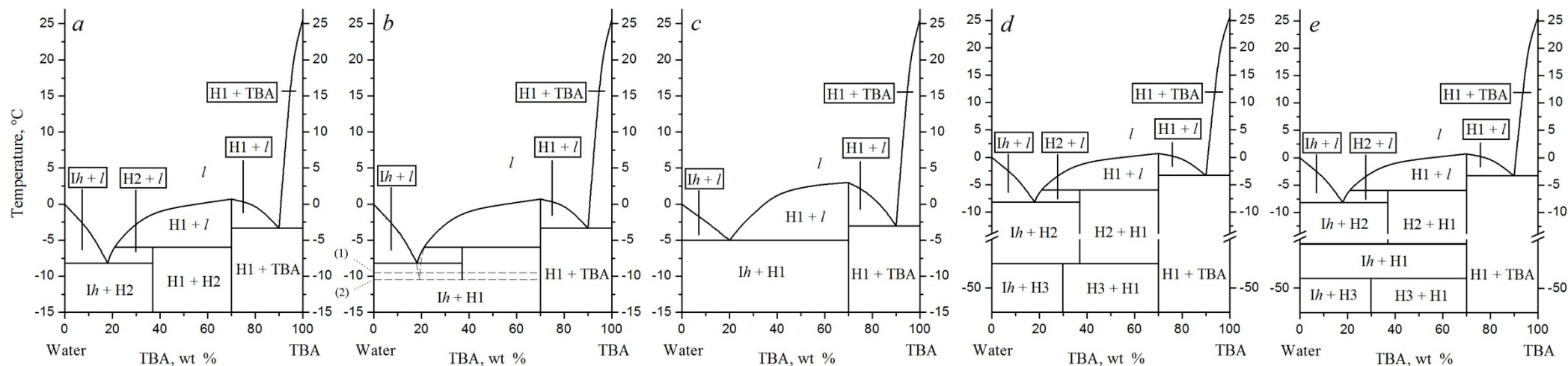


**Figure S1.** Several variants of the TBA – water system phase diagram based on the data of Rosso and Carbonnel, Ott *et al.*, Mootz and Staben (*a*)<sup>1-3</sup>, Rosso and Carbonnel, Mootz and Staben, Woznyj and Lüdemann (*b*)<sup>1,2,4</sup>, Kasraian and DeLuca (*c*)<sup>5</sup>. “Extended” variant based on data of Vessot and Andrieu, Kasraian and DeLuca, Dobrzycki<sup>5-7</sup> and our experimental (PXRD+TA) data (*d*) and a variant which can be realized at a higher pressure (*e*). Temperature of metastable *Ih*+H1 eutectic melting on (*b*): (1) – Rosso and Carbonnel,<sup>1</sup> Ott *et al.*<sup>2</sup> (2) – Woznyj and Lüdemann<sup>4</sup> (dashed lines).



## EXPERIMENTAL DETAILS

Analytical grade TBA, distilled water and D-(+)-trehalose dihydrate (for microbiology,  $\geq 99.0\%$ ; Sigma-Aldrich, Lot # BCBW5088) were used in this study.

### 1. Low-temperature PXRD (powder X-ray diffraction) experiments

PXRD experiments were carried out on a Bruker D8 Advance diffractometer ( $\lambda=1.5406 \text{ \AA}$ , tube voltage of 40 kV and tube current of 40 mA) equipped with an Anton Paar TTK 450 low temperature chamber. The vial with frozen solution was broken, the sample was gently ground in a mortar (all operations being performed at liquid nitrogen temperature) and placed onto a holder, which had been preliminary cooled to  $-100^\circ\text{C}$ .

Diffraction patterns were measured in the  $-100^\circ - -3^\circ\text{C}$  temperature range ( $2\Theta$  scans in the  $3^\circ - 42^\circ$  range, at  $0.02^\circ$  step, 0.1 sec/step).

### Samples for low-temperature powder X-ray diffraction

Starting TBA – water solutions: 10, 20, 29.8 (H3 composition), 37 (H2 composition), 55, 70 (H1 composition) and 85 wt % of TBA (Figure S1). All solutions were prepared by weighting components.

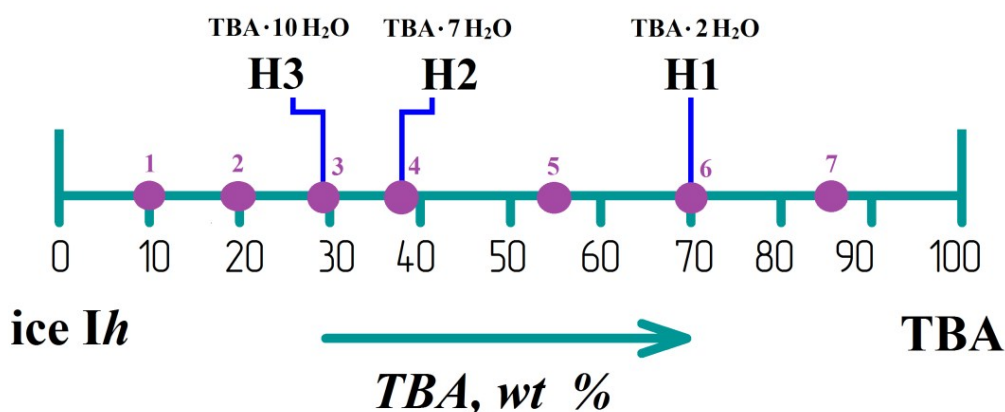


**Figure S2.** Samples (№№ 1-7) for low-temperature PXRD on water–TBA composition line.

Freezing protocols (as described in (Ogienko *et al.*, 2016)<sup>8</sup> (see Figure S3 for details)):

**Protocol I.** Vials (Sci/Spec, B69308), 1 ml aliquots, air thermostat,  $-20^\circ\text{C}$  (freezing time *ca.* 1 h).

**Protocol II.** Vials (Sci/Spec, B69308), 1 ml aliquots, cryothermostat (ethanol, KRYO-VT-05-02, TERMEX, Russia),  $-50^\circ\text{C}$  (freezing time *ca.* 3 min).

Immediately after freezing the solutions (protocols I, II) a few vials were broken under liquid nitrogen temperatures in order to extract the samples, which were after that kept in liquid nitrogen until diffraction experiments (hereafter ‘frozen’: Ia, IIa). The other vials of these series



were placed into an air thermostat at  $-20^{\circ}\text{C}$  for annealing (from 12 hours to 3 months) (hereafter ‘annealed’: Ib, IIb).

**Protocol III.** Small amounts of solution were splashed onto a copper plate cooled to liquid nitrogen temperature (freezing time *ca.* 1 sec). The frozen solution was gently ground manually at liquid nitrogen temperature. It was then divided into two parts. One part was kept in liquid nitrogen before diffraction experiments (hereafter ‘frozen’: IIIa), the other one was placed into an air thermostat at  $-20^{\circ}\text{C}$  for annealing (from 12 hours to 3 months) (hereafter ‘annealed’: IIIb).

To prepare samples according to “protocol III” for measurements of sublimation rate and determination of sublimation behavior of TBA hydrates, vials with TBA – water solution (29.8 wt % of TBA) were frozen in a vessel with liquid nitrogen (hereafter: IIIa\_vial) and placed into an air thermostat at  $-20^{\circ}\text{C}$  for annealing (12 hours) (hereafter: IIIb\_vial).

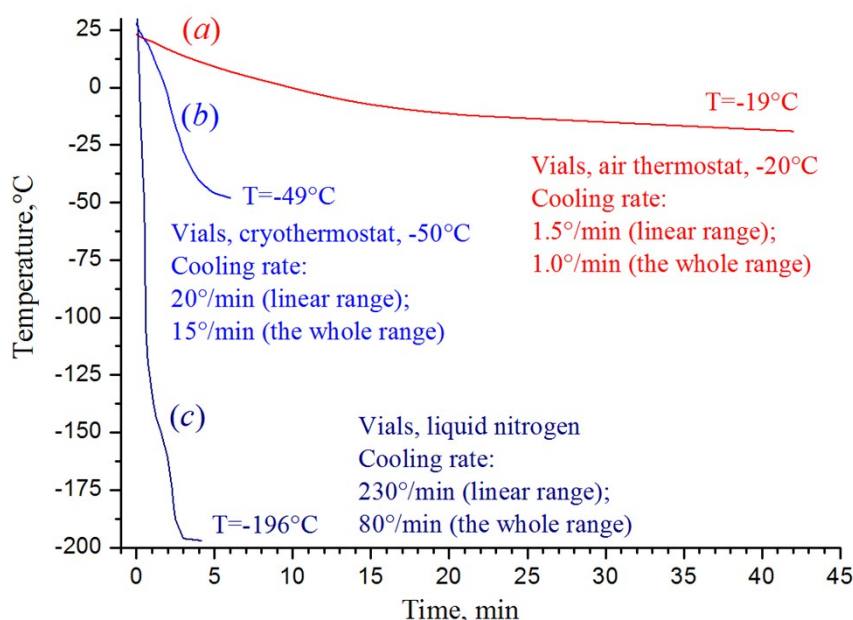


**Figure S3.** Estimated cooling rates corresponding to different freezing protocols. *a* – vials in an air thermostat (protocol Ia),  $-20^{\circ}\text{C}$ ; *b* – vials in a cryothermostat at  $-50^{\circ}\text{C}$  (protocol IIa); *c* – vials in a vessel with liquid nitrogen (protocol IIIa\_vial).

## 2. DSC experiments

Low-temperature DSC experiments were carried out using a DSC 204 F1 Phoenix (Netzsch), in a flow of dry argon (25 ml/min). The drop of the hot solution ( $+30^{\circ}\text{C}$ ) was placed into a crucible (which was immediately sealed) and cooled down to  $-50^{\circ}\text{C}$  at a cooling rate of  $1^{\circ}/\text{min}$  (no measurements on cooling), and then heated (with measurements from  $-40^{\circ}\text{C}$  to  $50^{\circ}\text{C}$ ) at the heating rate of  $6^{\circ}/\text{min}$ , similar to other samples.

### 3. TA experiments

The TA experiments were carried out using a home-made instrument described in (Ogienko *et al.*, 2018).<sup>9</sup> The temperature of a sample was registered using a precision converter of signals of resistance thermometers and thermocouples "TERCON" with a multiplex switch of input signals "TERCON-K" (TERMEX, Tomsk, Russia). The assembly of samples was placed into an autoclave. Then, the autoclave was cooled/heated ( $+25^{\circ}\text{C} \rightarrow -20^{\circ}\text{C}$  (exposure for 30 min.)  $\rightarrow +25^{\circ}\text{C}$ ) at the constant rates of 0.35 or  $1.5^{\circ}\text{C}/\text{min}$  at atmospheric pressure. The absolute temperature uncertainty was  $\pm 0.2^{\circ}\text{C}$ .

Loading methods:

#### 1. "Conventional loading"

Each aluminum sample holder was loaded with four PTFE cells filled with solutions (10, 20, 29.8, 37 and 55 wt % of TBA; the volume of the samples were 1.000 ml; the thickness of the solution layer in each of the cells was 13 mm). Type K thermocouple was placed in each of the samples, the junction being approximately in the middle of the sample.

#### 2. "Cold loading"

Samples of frozen solution (29.8 wt % of TBA, prepared according to protocol IIIa) were ground in a metal mortar cooled to liquid nitrogen temperature and then loaded into PTFE cells (the thickness of the frozen formulation layer in each cell was  $\sim 13\text{-}15$  mm.), which were placed into aluminum sample holders. All the parts of the TA instrument were also cooled to liquid nitrogen temperature. A type K thermocouple precooled to liquid nitrogen temperature was placed into each sample. The assembly of samples was placed into a thermostat bath precooled to  $0^{\circ}\text{C}$  and maintained at this temperature of circulating coolant (ethanol) during all the experiment.

### 4. Measurements of the sublimation rate

Measurements of the sublimation rate were accomplished with a laboratory-scale freeze-dryer (one processing shelf made of polished stainless steel,  $25.0 \times 35.0$  cm; the temperature of the shelf can be varied from  $-35^{\circ}\text{C}$  to  $80^{\circ}\text{C}$ ) (NIIC SB RAS, Russia) equipped with an organic solvent trap.<sup>8</sup> Two convection-enhanced Pirani gauges (275 Mini-Convectron® (Granville-Phillips®)) were used to monitor the chamber and condenser pressure. The operating pressure was regulated with a dry nitrogen injection through a micro valve to the chamber.

All the experiments were carried out with 15-ml injection vials made of colorless borosilicate glass tubing and 13-mm 2 leg freeze-drying stoppers (Jiagsu Runde Ltd., China). All vials with TBA – water solution (29.8 wt % of TBA) were numbered and weighed ( $2.000 \pm 0.005$  g in each vial) before an experiment (12 vials total in a series, including 10 vials for an experiment itself and 2 vials for PXRD, to identify the phases formed on freezing/annealing). The vials were frozen or frozen/annealed (according to protocols "Ia" and "IIIb\_vial" as described above) and placed on the precooled shelf ( $-10^{\circ}\text{C}/-25^{\circ}\text{C}$ ) without having contact with each other. KPT-8 contact paste (Solins, Russia) consisting of silicon with

zinc oxide was used to enhance the heat transfer (heat conductivity of 1.0-0.7 W/mK in the temperature region of -50 - 20°C). All the experiments were performed at a chamber pressure of 100±10 mTorr (to maintain the temperature of the sample just below (Chang and Fischer, 1995)<sup>10</sup>  $T_g'$  value for frozen trehalose solution (~-30°C) (Her and Nail, 1994)<sup>11</sup>. The experiment was terminated by breaking vacuum in a predetermined time after which the vials were reweighed. The experiments were repeated for different periods of drying.

#### 5. Determination of the sublimation behavior of TBA hydrates

Experiments aimed to determine the sublimation behavior of TBA hydrates were performed with the use of the laboratory scale freeze-dryer and vials described above.

Two types of experiments were performed:

##### 1. “Lyophilization in vials”

Vials were filled with 2.000±0.005 g of TBA – water solution (29.8 wt % of TBA, H3 composition, frozen or frozen/annealed according to protocols: “Ia”, “IIIa\_vial”, “IIIb\_vial”) and placed on the precooled shelf (-10°C) without having contact with each other. 5 vials total were used in each series, including 4 vials for the experiment itself and a vial for PXRD, in order to identify the phases formed on freezing/annealing. All the experiments were performed at chamber pressure of 100±10 mTorr. After removing ~50% of the sample, the experiment was terminated and vials were frozen immediately in a vessel with liquid nitrogen. After that the vials were broken, the frozen samples were gently ground and stored until diffraction experiments (all listed stages were carried out under liquid nitrogen temperature).

##### 2. An “*in situ*” diffraction experiment at ambient and reduced pressure

Three vials were filled with 2.000±0.005 g of TBA – water solution (29.8 wt % of TBA, H3 composition, frozen or frozen/annealed according to protocols: “Ia”, “IIIa\_vial”, “IIIb\_vial”). The vials were broken and the frozen samples were gently ground at liquid nitrogen temperature. Then, they were placed onto a holder, which had been preliminary cooled to -100°C. Diffraction patterns were measured at -100°C/ambient pressure. Then, the sample holder was heated to -10°C at 100 mTorr. Diffraction pattern were measured every 10 minutes after reaching the required temperature until the sample was completely removed by sublimation.

#### 6. Scanning electron microscopy (SEM)

Morphological examination of the surface and internal structure of trehalose freeze-dried cakes was carried out using a TM-1000 (Hitachi) scanning electron microscope. The samples were mounted on a metal stub with double-sided adhesive tape and coated with gold to a thickness of about 8 nm using a Jeol JFC-1600 Auto Fine Coater.

**Extended version of Table 2 in main text.** Results of the low-temperature PXRD experiments aimed at identifying the phases formed on freezing and subsequent annealing in the TBA–water system. Annealing defines heating the sample from the freezing temperature to -20°C and keeping at these conditions up to 3 months. The main phase of the sample is indicated first. The admixture phases (giving a few weak reflections on PXRD patterns) are shown in brackets.

Freezing protocol	TBA, wt %						
	10%	20%	29.8 (H3)	37% (H2)	55%	70% (H1)	85%
Ia	Ih+H1	Ih+H1	H1+Ih	H1+Ih	H1+Ih	H1 [TBA]	H1+TBA
Ib	Ih+H2	Ih+H2	H2+Ih	H2 [Ih + H1]	H1+H2	H1 [H2]	H1+TBA
IIa	Ih+H1	Ih+H3 [H2]	H3+Ih	H1+Ih [H3]	H1+Ih	H1 [Ih]	H1+TBA
IIb	Ih+H2	Ih+H2	H2+Ih	H2 [Ih + H1]	H1+H2 [Ih]	H1 [TBA]	H1+TBA
IIIa	Ih+H1	H3+Ih	H3	H1+H3	H1 [H3]	H1 [TBA]	H1+TBA
IIIb	Ih+H2	Ih+H2	H2+Ih	H2 [Ih]	H1+H2	H1	H1+TBA

The annealing protocols are relevant for actual freeze-drying operations used in industry. This is especially true for the freezing in vials.

In a general case, the annealing stage can be used for the following purposes: (1) to eliminate metastable phases, which have been formed on fast cooling of solutions; (2) to achieve crystallization of a solute (crystalline API or bulking agent); (3) to modify the morphology of the ice crystals (increase their size). The last two points are very important for the freeze-dried pharmaceutical/biopharmaceutical drug formulations, since they help to improve the stability of the product, allow one to decrease the amount of the residual solvents (point 2), and also shorten the primary drying stage by decreasing the dried layer resistance (point 3) when larger pores are formed on sublimation of larger ice crystals.

In the case described in this manuscript, after a rather fast and deep cooling, the temperature was set a little bit higher than  $T_g'$  (~-32°C), but not exceeding the eutectic melting temperature (which is equal to -

10.5°C for the metastable  $I_h+H_1$  eutectic (Woznyj and Lüdemann).<sup>4</sup> The value of -20°C is this intermediate value between the eutectic melting temperature and the  $T_g'$ .

More details about the choice of the annealing temperature are given in (Tang and Pikal)<sup>12</sup>:

“Normal Freezing Process for Amorphous Products”:

1. Load vials onto the shelf and allow to come to 5°C; hold for 15 to 30 min.
2. Cool to -5°C without ice formation and hold for 15 to 30 min (this normally results in improved homogeneity of crystallization, both intra- and inter-vial).
3. Decrease the shelf temperature to a final shelf temperature of -40°C (all solutes in solid state) at about 1°C/min.
4. Hold for 1 h if fill depth is less or equal to 1 cm or 2 h if the fill depth is greater than 1 cm.

“Thermal Cycle To Achieve Solute Crystallization (Crystalline Drug or Bulking Agent)”:

1. Step 1 to 3 as above.
2. Bring product temperature to 10 to 20°C above  $T_g'$  but well below the onset of eutectic melt and hold for several hours.
3. Steps 3 and 4 as above freezing process for amorphous products.

## RESULTS

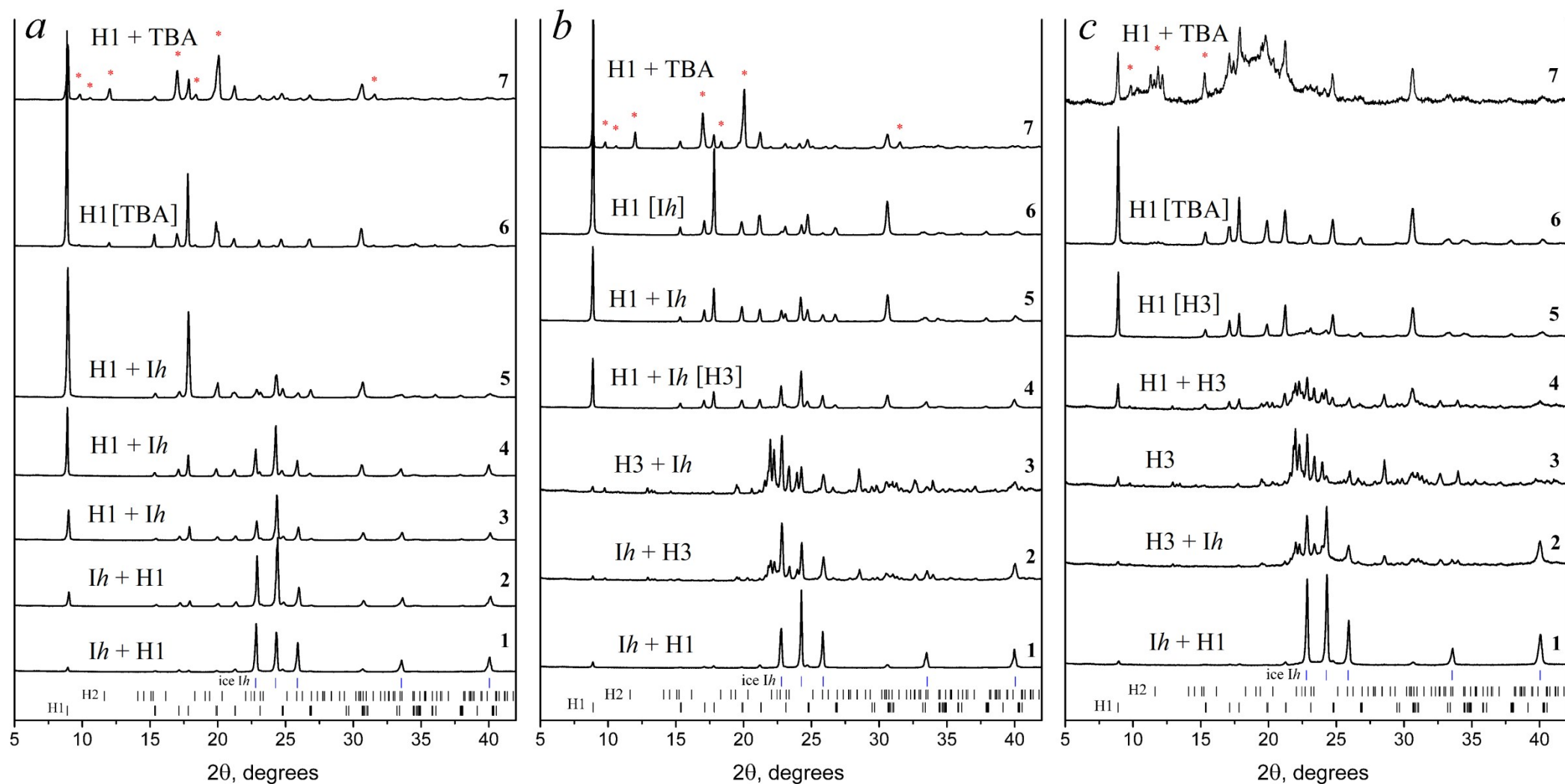


**Figure S4.** PXRD patterns of frozen TBA–water solutions recorded at  $-100^{\circ}\text{C}$  (a – protocol Ia, b – protocol IIa, c – protocol IIIa). The positions of reflections of the TBA hydrates (H1 and H2) and ice Ih are shown as ticks at the bottom. The positions of reflections of the H3 are not shown for clarity. \* – the strongest reflections of the TBA. 1, 2, 3, 4, 5, 6, 7 – correspond to 10, 20, 29.8 (H3), 37 (H2), 55, 70 (H1) and 85 wt % of TBA, respectively. The admixture phases (a few weak reflections on PXRD patterns) are shown in brackets.

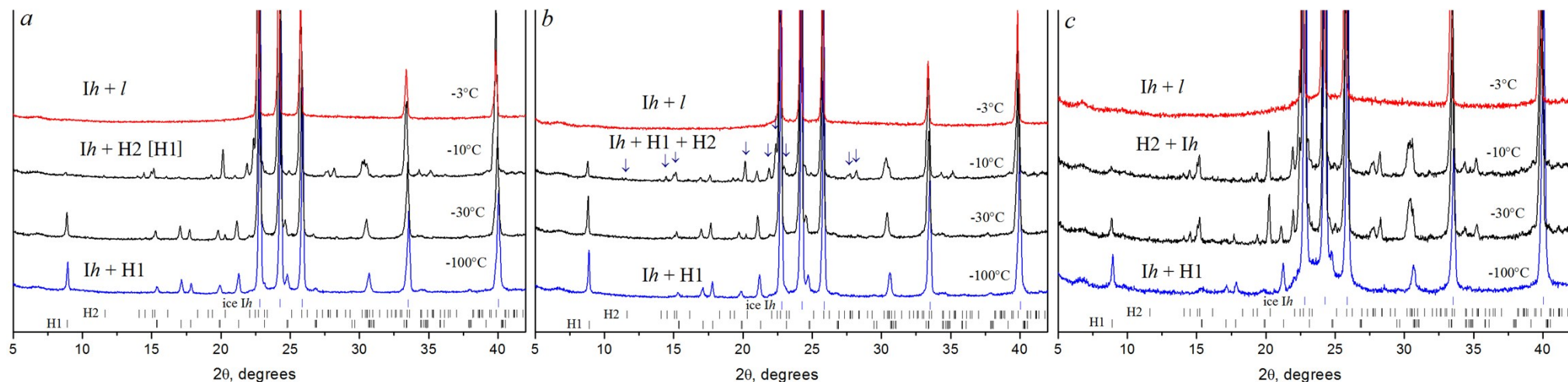


**Figure S5.** PXRD patterns of frozen TBA–water solutions (10 wt % of TBA) at different temperatures (*a* – protocol Ia, *b* – protocol IIa, *c* – protocol IIIa). The positions of reflections of the TBA hydrates (H1 and H2) and ice  $I_h$  are shown as ticks at the bottom. The strongest reflections of the H2 (figure *b*) are pointed by arrows. The admixture phases (a few weak reflections on PXRD patterns) are shown in brackets.

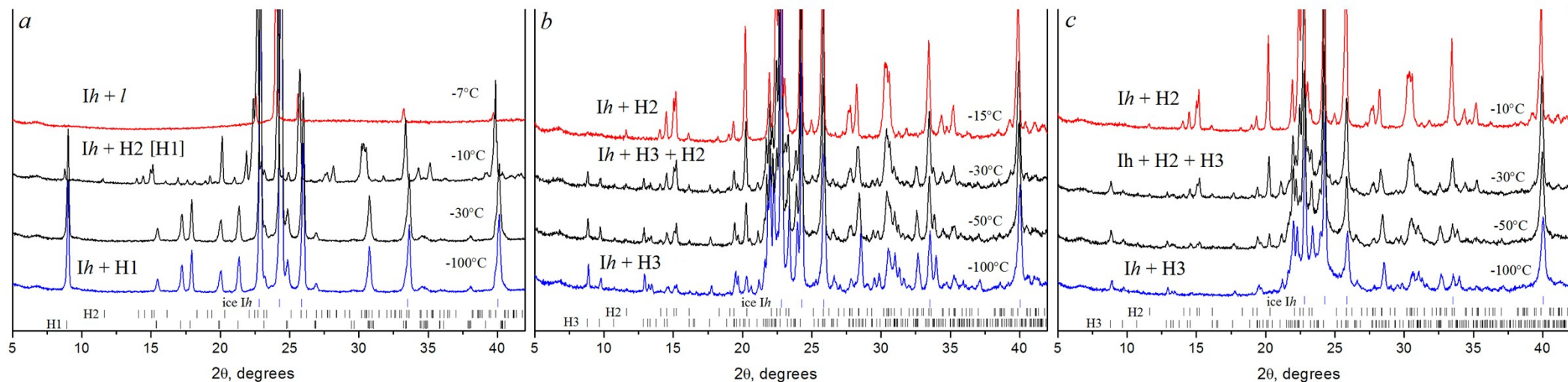


**Figure S6.** PXRD patterns of frozen TBA–water solutions (20 wt % of TBA) at different temperatures (*a* – protocol Ia, *b* – protocol IIa, *c* – protocol IIIa). The positions of reflections of the TBA hydrates (H1, H2, H3) and ice  $I_h$  are shown as ticks at the bottom. The admixture phases (a few weak reflections on PXRD patterns) are shown in brackets.



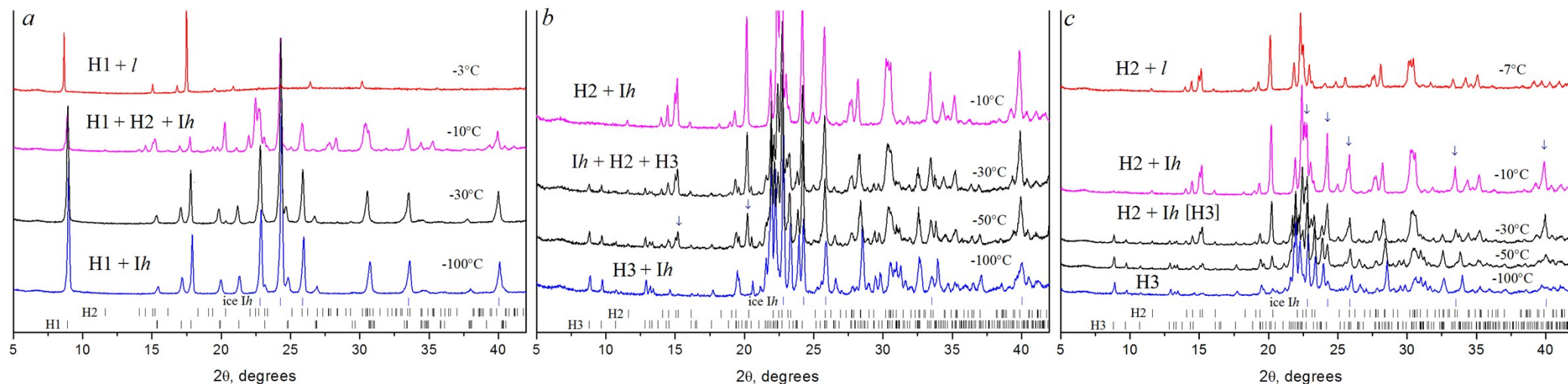


**Figure S7.** PXRD patterns of frozen TBA–water solutions (29.8 wt % of TBA, H3 composition) at different temperatures (*a* – protocol Ia, *b* – protocol IIa, *c* – protocol IIIa). The positions of reflections of the TBA hydrates (H1, H2, H3) and ice *Ih* are shown as ticks at the bottom. The strongest reflections of the H2 (figure *b*) and ice *Ih* (figure *c*) phases are pointed by navy arrows. The admixture phases (a few weak reflections on PXRD patterns) are shown in brackets.

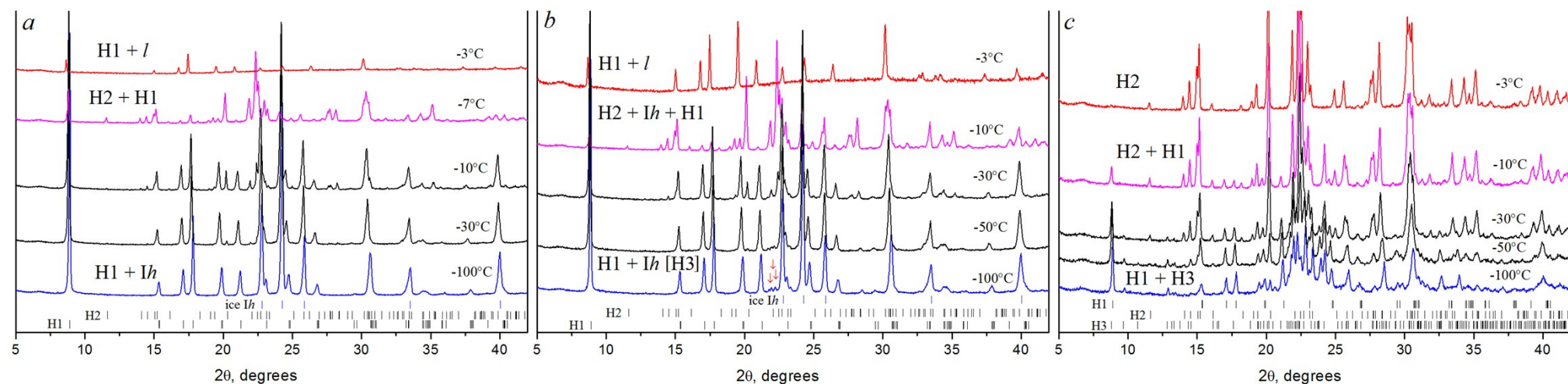


**Figure S8.** PXRD patterns of frozen TBA–water solutions (37 wt % of TBA, H2 composition) at different temperatures (*a* – protocol Ia, *b* – protocol IIa, *c* – protocol IIIa). The positions of reflections of the TBA hydrates (H1, H2, H3) and ice *Ih* are shown as ticks at the bottom. The strongest reflections of the unidentified phase (H3) (figure *b*) are pointed by red arrows. The admixture phases (a few weak reflections on PXRD patterns) are shown in brackets.

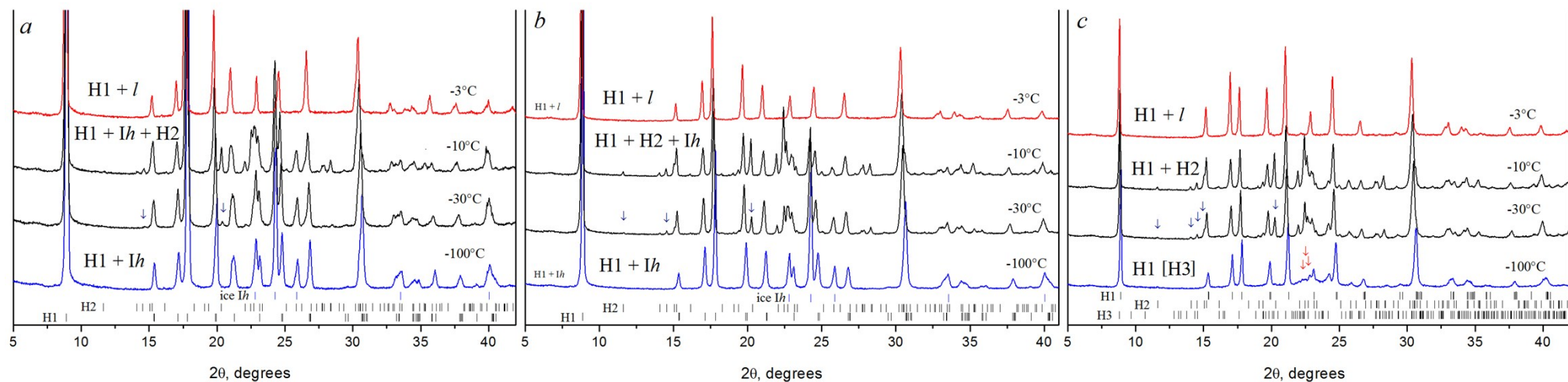


**Figure S9.** PXRD patterns of frozen TBA–water solutions (55 wt % of TBA) at different temperatures (*a* – protocol Ia, *b* – protocol IIa, *c* – protocol IIIa). The positions of reflections of the TBA hydrates (H1, H2, H3) and ice Ih are shown as ticks at the bottom. The strongest reflections of the unidentified phase (H3) (figure *c*) are pointed by red arrows. The appearance of H2 reflections pointed by navy arrows. The admixture phases (a few weak reflections on PXRD patterns) are shown in brackets.

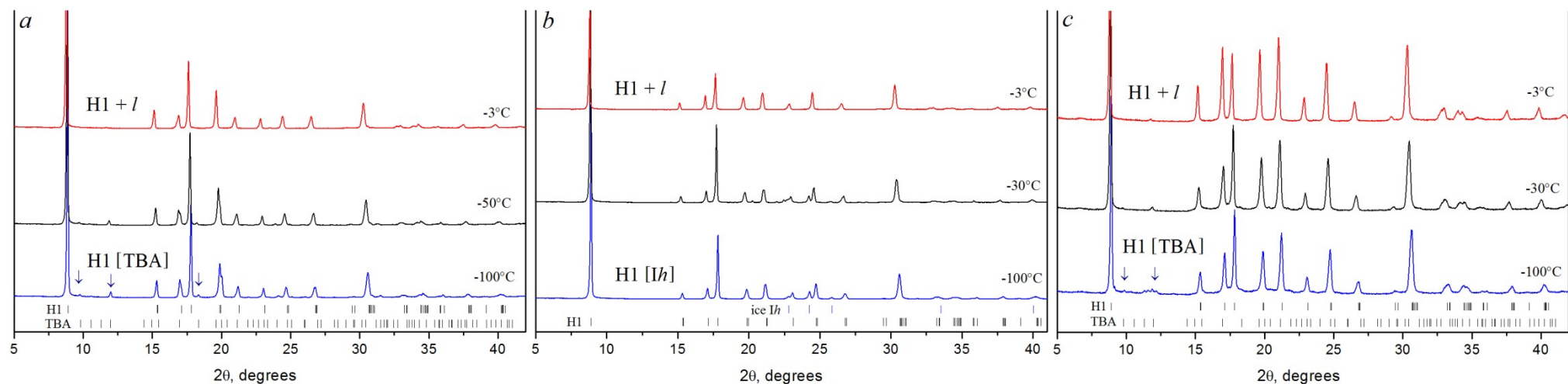


**Figure S10.** PXR D patterns of frozen TBA – water solutions (70 wt % of TBA, H1 composition) at different temperatures (*a* – protocol Ia, *b* – protocol IIa, *c* – protocol IIIa). The positions of reflections of the H1 TBA hydrate and TBA are shown as ticks at the bottom. The strongest reflections of the TBA (figures *a* and *c*) are pointed by navy arrows. The admixture phases (a few weak reflections on PXR D patterns) are shown in brackets.

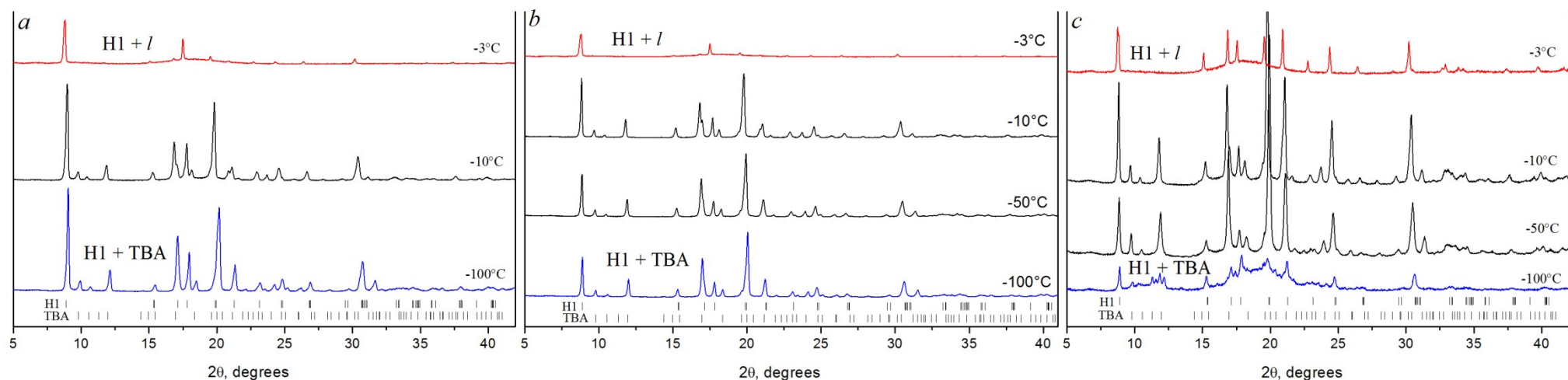


**Figure S11.** PXR D patterns of frozen TBA – water solutions (85 wt % of TBA) at different temperatures (*a* – protocol Ia, *b* – protocol IIa, *c* – protocol IIIa). The positions of reflections of the H1 TBA hydrate and TBA are shown as ticks at the bottom.

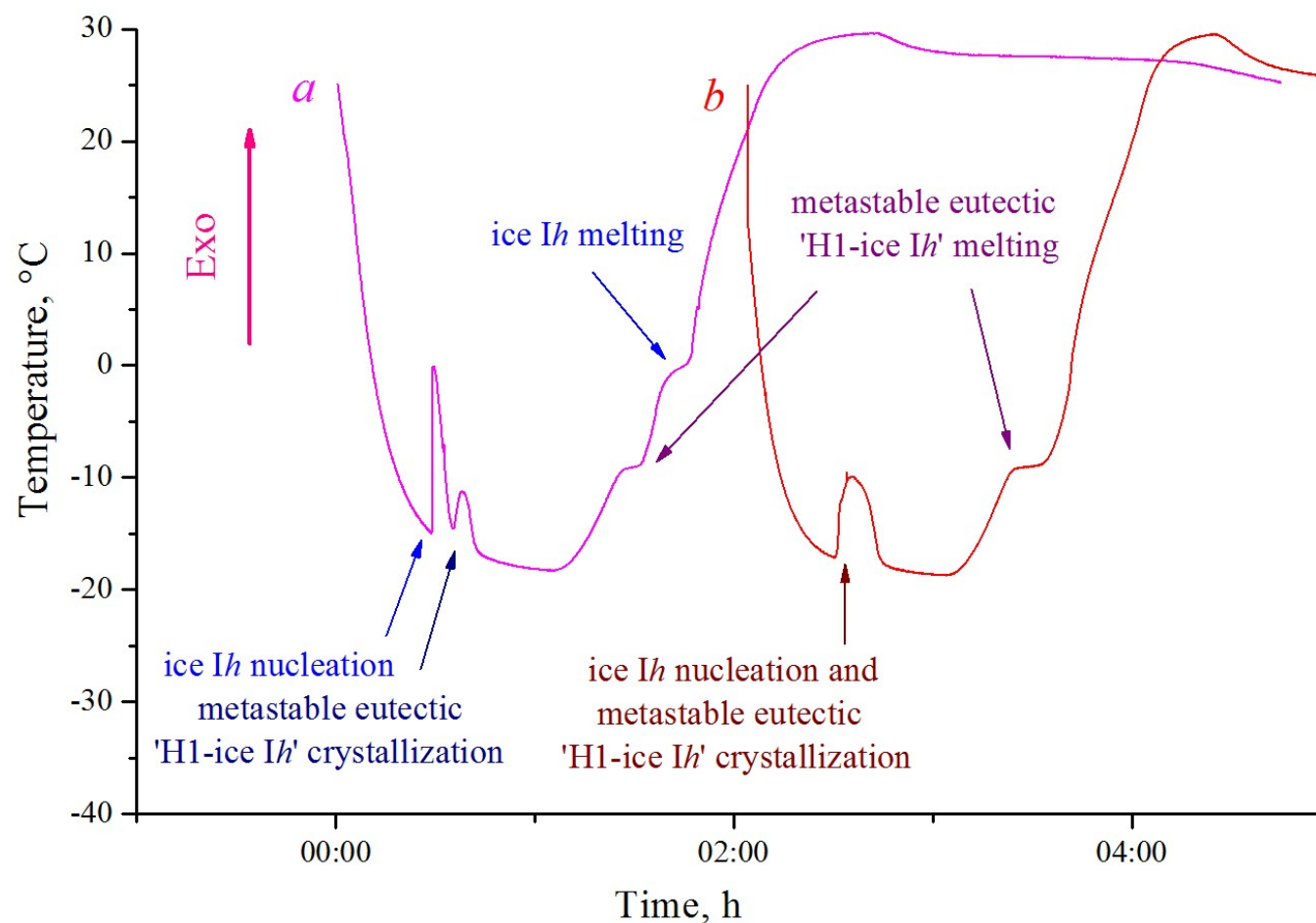


**Figure S12.** Typical experimental curves obtained in TA experiments (cooling and subsequent heating). Cooling rate of  $\sim 1^{\circ}\text{C}/\text{min}$  (similar to protocol Ia). *a* (magenta line) – 10 wt % of TBA, *b* (red line) – 29.8 wt % of TBA (H3 composition).



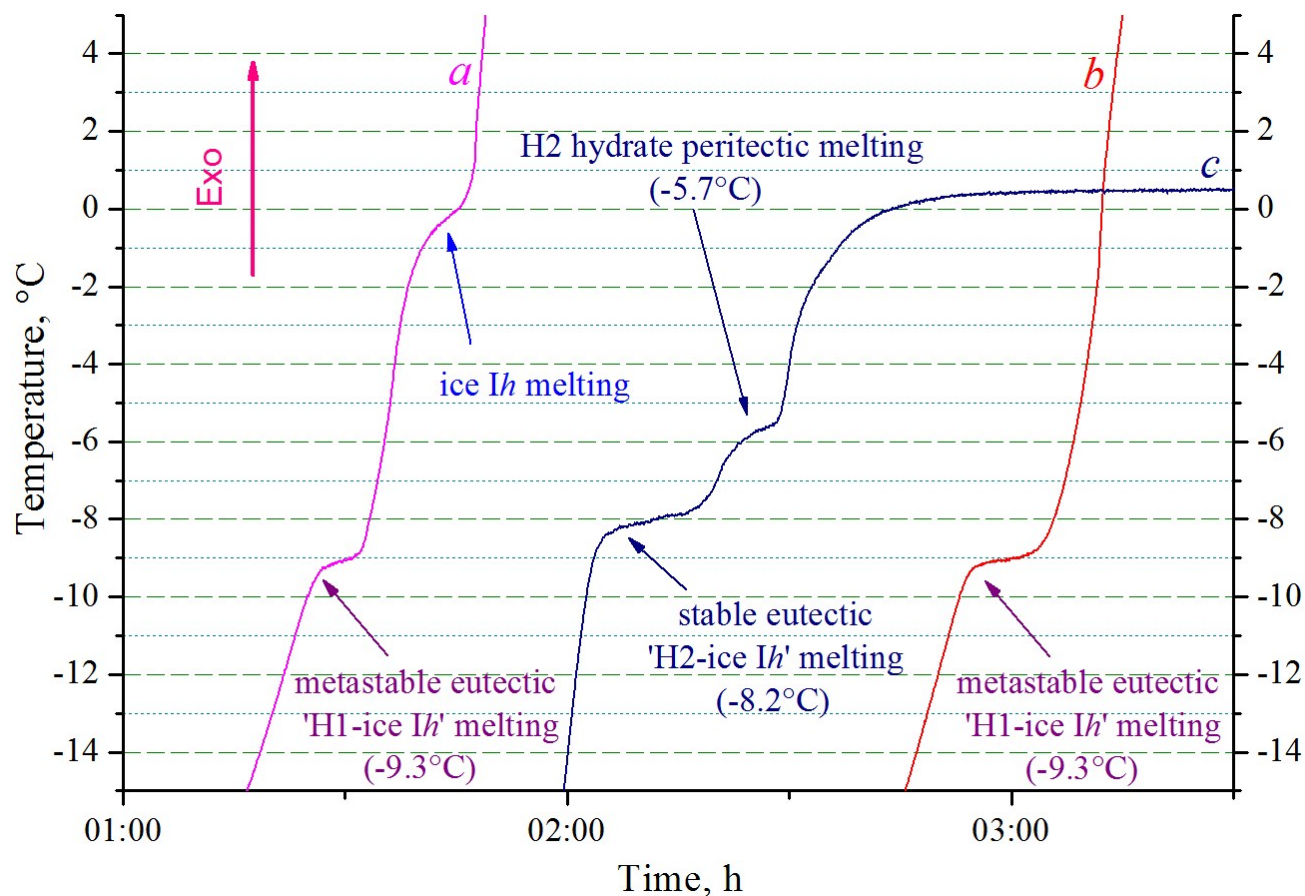


**Figure S13.** Comparison of thermal effects, obtained in TA experiments (on heating) for samples of solutions frozen according to protocol Ia (*a* (magenta line) – 10 wt % of TBA; *b* (red line) – 29.8 wt % of TBA) and protocol IIIa (“cold loading”, *c* (navy line) – 29.8 wt % of TBA).

The TA curve measured on heating the solution of H3 composition (29.8 wt % of TBA) frozen according to protocol IIIa (*c*) shows two thermal effects at -8.2 and -5.7°C that agrees well with data of (Rosso and Carbonnel, 1968; Ott *et al.*, 1979; Mootz and Staben, 1993)<sup>1-3</sup> and corresponds to the “H2+Ih” eutectic melting ( $Ih + H2 = l$ ) and to the incongruent melting of H2 ( $H2 = H1 + l$ ). On TA curves measured on heating the solutions frozen according to protocol Ia (*a*, *b*) show thermal effect at -9.3°C that corresponds to the “H1+Ih” metastable eutectic melting ( $Ih + H1 = l$ ).

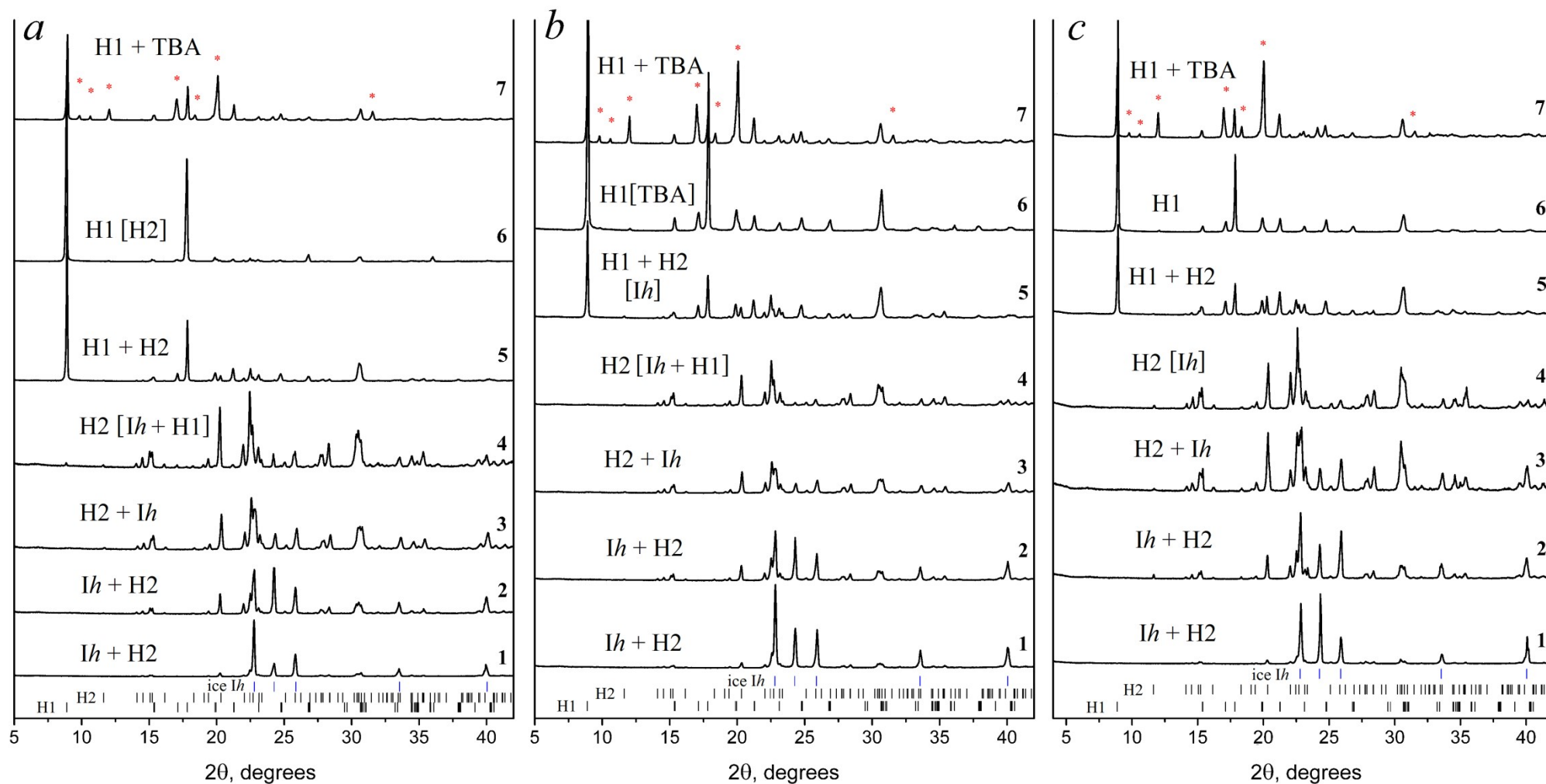


**Figure S14.** PXR D patterns of frozen and subsequently annealed TBA–water solutions recorded at  $-100^{\circ}\text{C}$  (*a* – protocol I*b*, *b* – protocol II*b*, *c* – protocol III*b*). The positions of reflections of the TBA hydrates (H1 and H2) and ice *Ih* are shown as ticks at the bottom. \* - the strongest reflections of the TBA. 1, 2, 3, 4, 5, 6, 7 – correspond to 10, 20, 29.8 (H3), 37 (H2), 55, 70 (H1) and 85 wt % of TBA, respectively. The admixture phases (a few weak reflections on PXR D patterns) are shown in brackets.



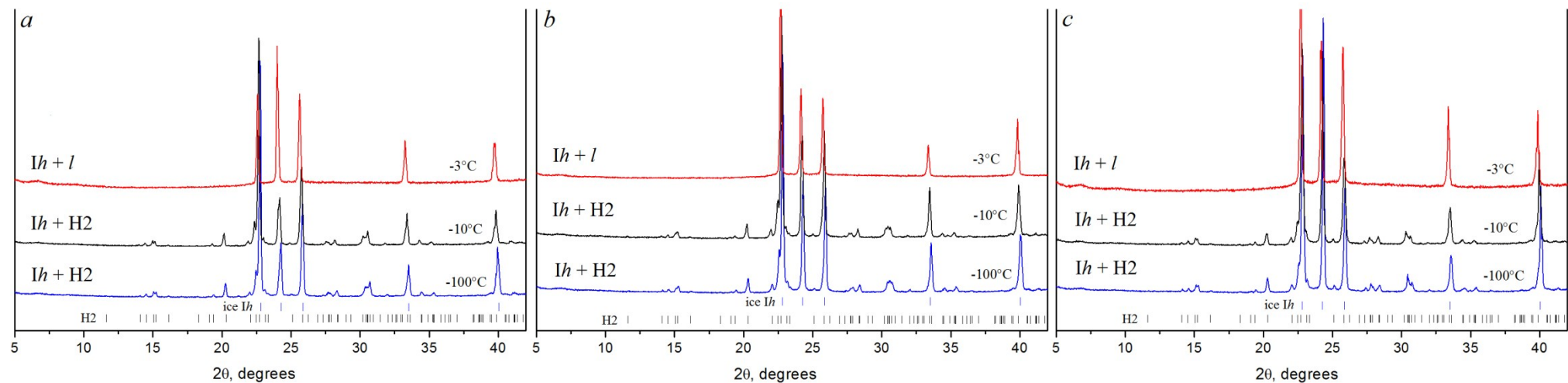


**Figure S15.** PXRD patterns of frozen and subsequently annealed TBA–water solutions (10 wt % of TBA) at different temperatures (*a* – protocol Ib, *b* – protocol IIb, *c* – protocol IIIb). The positions of reflections of the H2 and ice Ih are shown as ticks at the bottom.

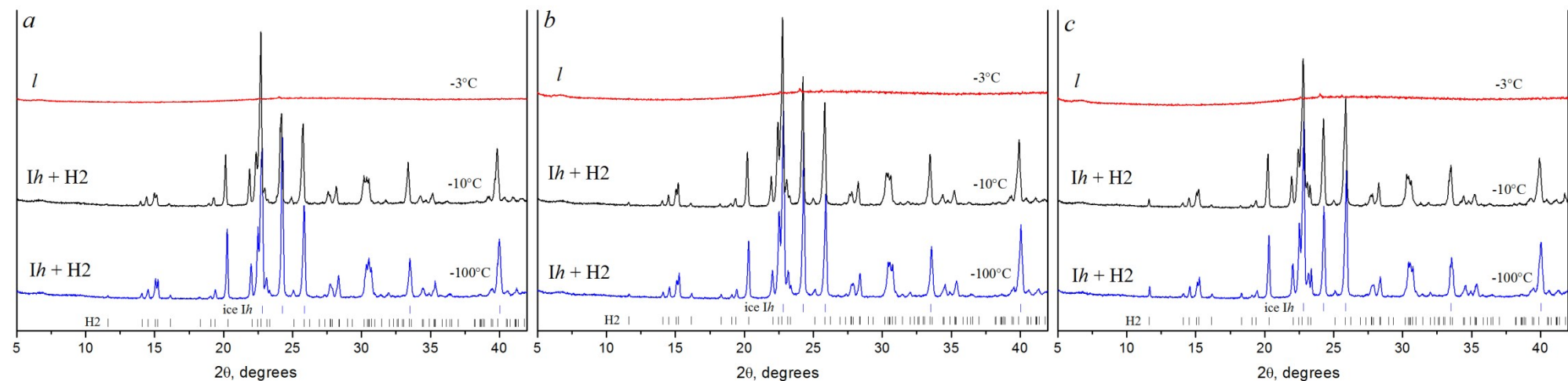


**Figure S16.** PXRD patterns of frozen and subsequently annealed TBA–water solutions (20 wt % of TBA) at different temperatures (*a* – protocol Ib, *b* – protocol IIb, *c* – protocol IIIb). The positions of reflections of the H2 and ice Ih are shown as ticks at the bottom.

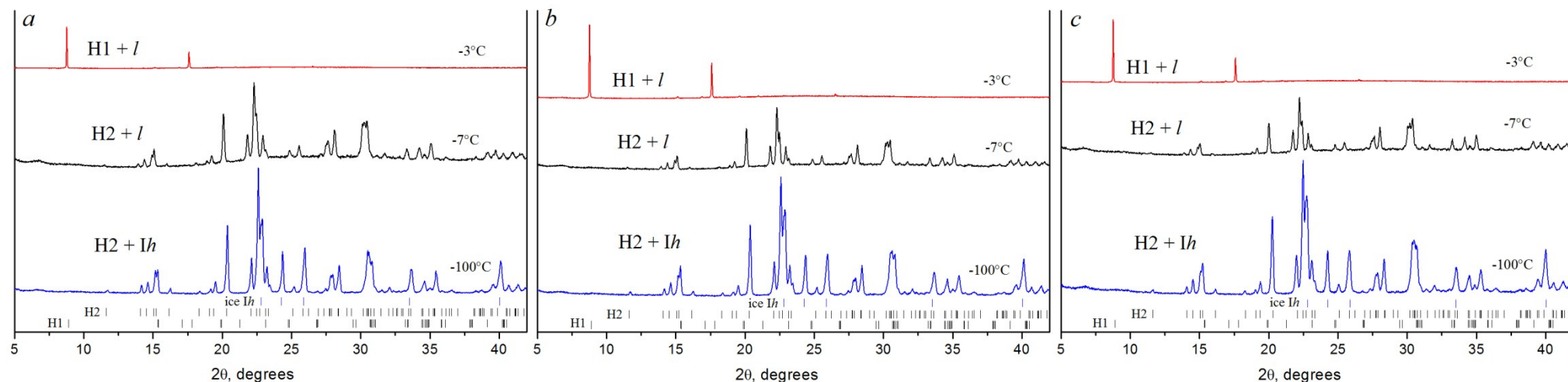


**Figure S17.** PXRD patterns of frozen and subsequently annealed TBA–water solutions (29.8 wt % of TBA, H3 composition) at different temperatures (*a* – protocol Ib, *b* – protocol IIb, *c* – protocol IIIb). The positions of reflections of the TBA hydrates (H1, H2) and ice Ih are shown as ticks at the bottom.

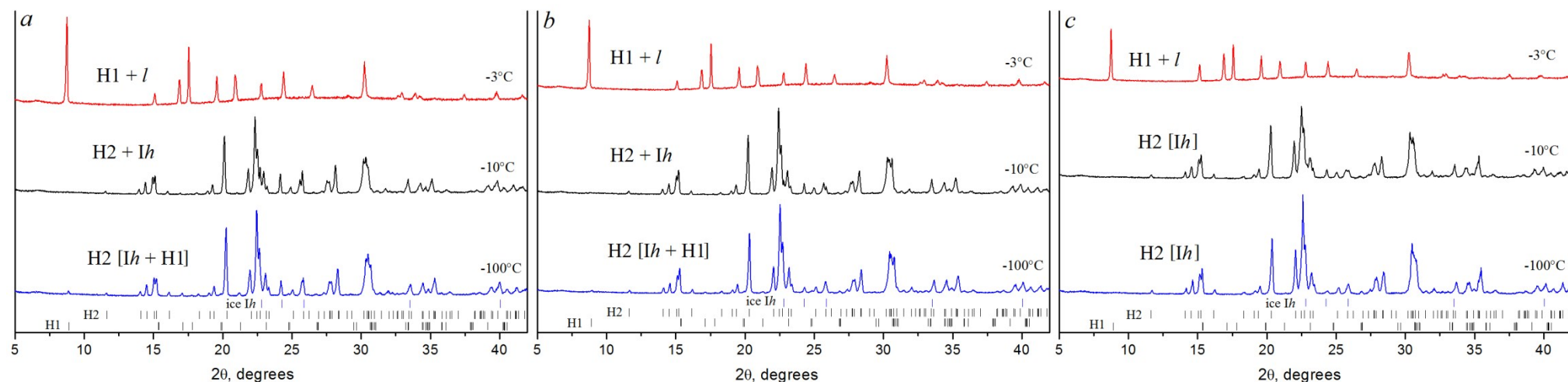


**Figure S18.** PXRD patterns of frozen and subsequently annealed TBA–water solutions (37 wt % of TBA, H2 composition) at different temperatures (*a* – protocol Ib, *b* – protocol IIb, *c* – protocol IIIb). The positions of reflections of the TBA hydrates (H1, H2) and ice Ih are shown as ticks at the bottom. The admixture phases (a few weak reflections on PXRD patterns) are shown in brackets.

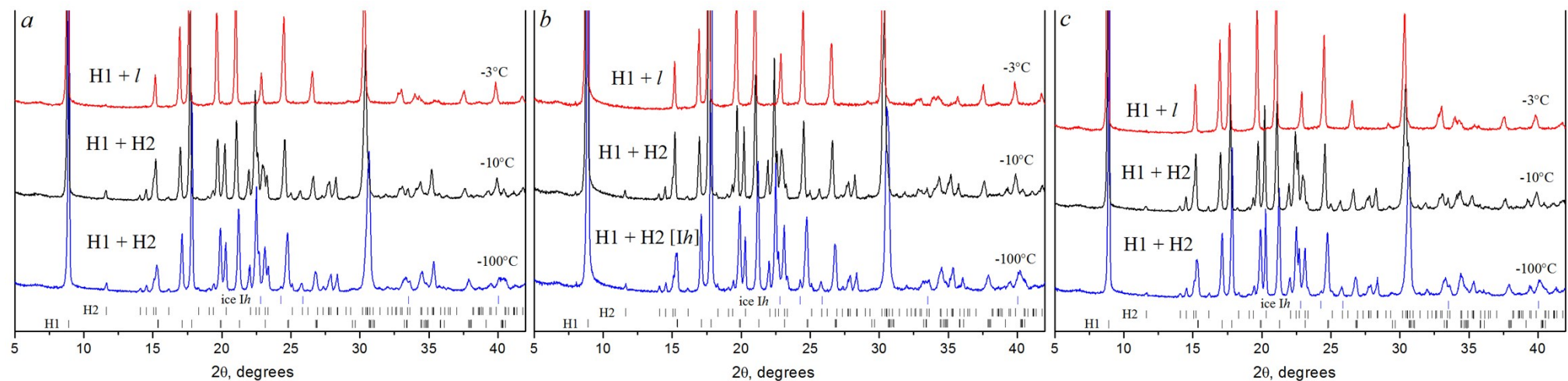


**Figure S19.** PXRD patterns of frozen and subsequently annealed TBA–water solutions (55 wt % of TBA) at different temperatures (*a* – protocol Ib, *b* – protocol IIb, *c* – protocol IIIb). The positions of reflections of the TBA hydrates (H1, H2) and ice *Ih* are shown as ticks at the bottom. The admixture phases (a few weak reflections on PXRD patterns) are shown in brackets.

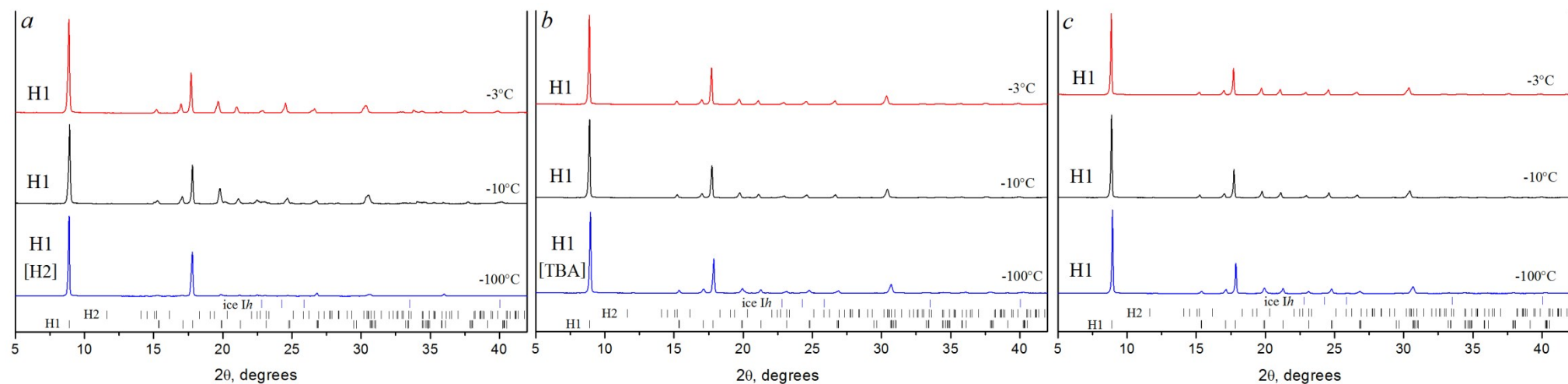


**Figure S20.** PXRD patterns of frozen and subsequently annealed TBA–water solutions (70 wt % of TBA, H1 composition) at different temperatures (*a* – protocol Ib, *b* – protocol IIb, *c* – protocol IIIb). The positions of reflections of the TBA hydrates (H1, H2) and ice *Ih* are shown as ticks at the bottom. The admixture phases (a few weak reflections on PXRD patterns) are shown in brackets.

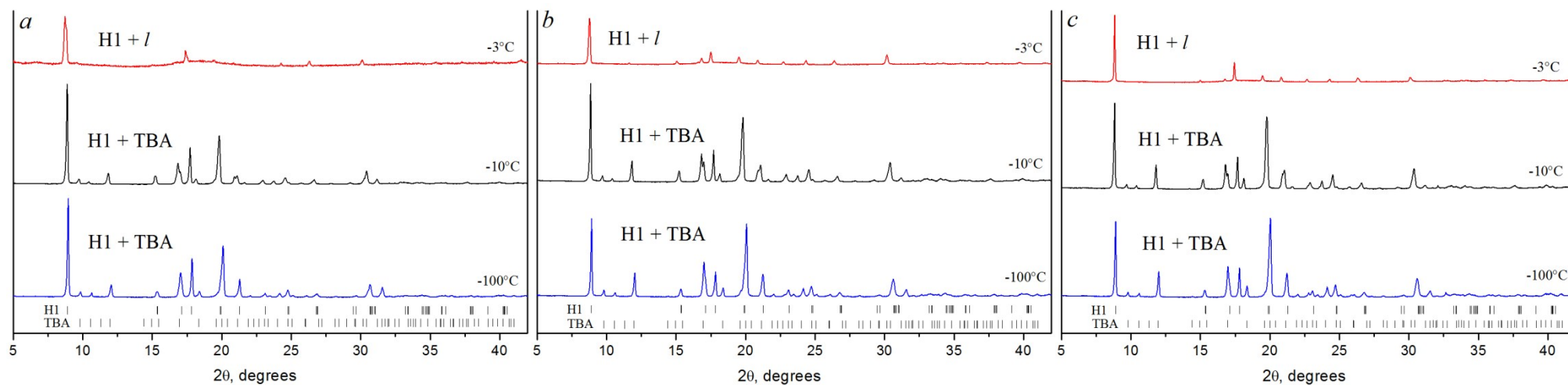


**Figure S21.** Powder diffraction patterns of frozen and subsequently annealed TBA–water solutions (85 wt % of TBA) at different temperatures (*a* – protocol Ib, *b* – protocol IIb, *c* – protocol IIIb). The positions of reflections of the H1 and TBA are shown as ticks at the bottom.

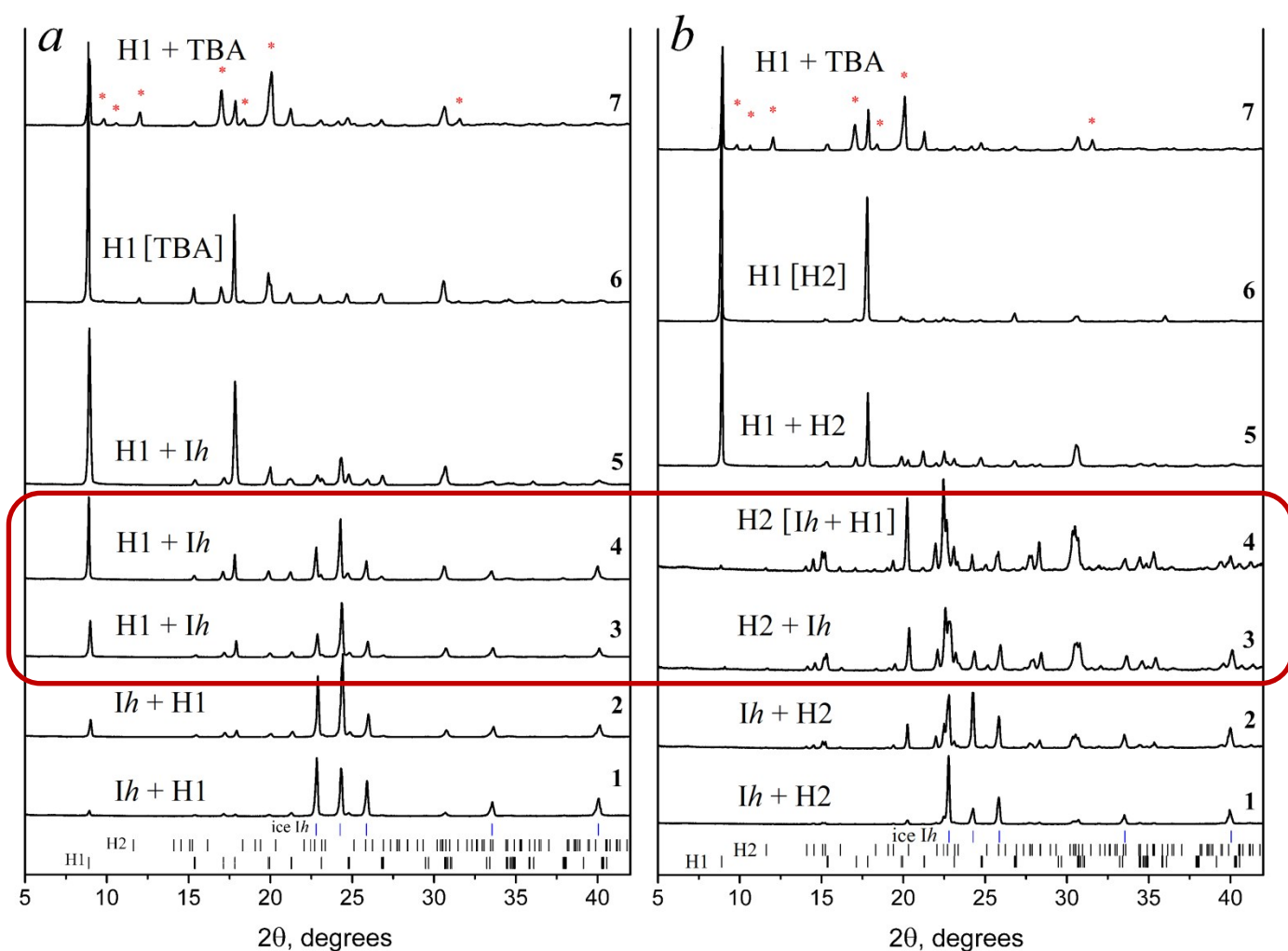


**Figure S22.** Comparison of PXRD patterns of frozen (*a* – protocol Ia) and subsequently annealed (*b* – protocol Ib) TBA – water solutions recorded at  $-100^{\circ}\text{C}$ . The positions of reflections of the TBA hydrates (H1 and H2) and ice *Ih* are shown as ticks at the bottom. The positions of reflections of the H3 are neglected for clarity. \* – the strongest reflections of the TBA. 1, 2, 3, 4, 5, 6, 7 – correspond to 10, 20, 29.8 (H3), 37 (H2), 55, 70 (H1) and 85 wt % of TBA, respectively. The admixture phases (a few weak reflections on PXRD patterns) are shown in brackets.



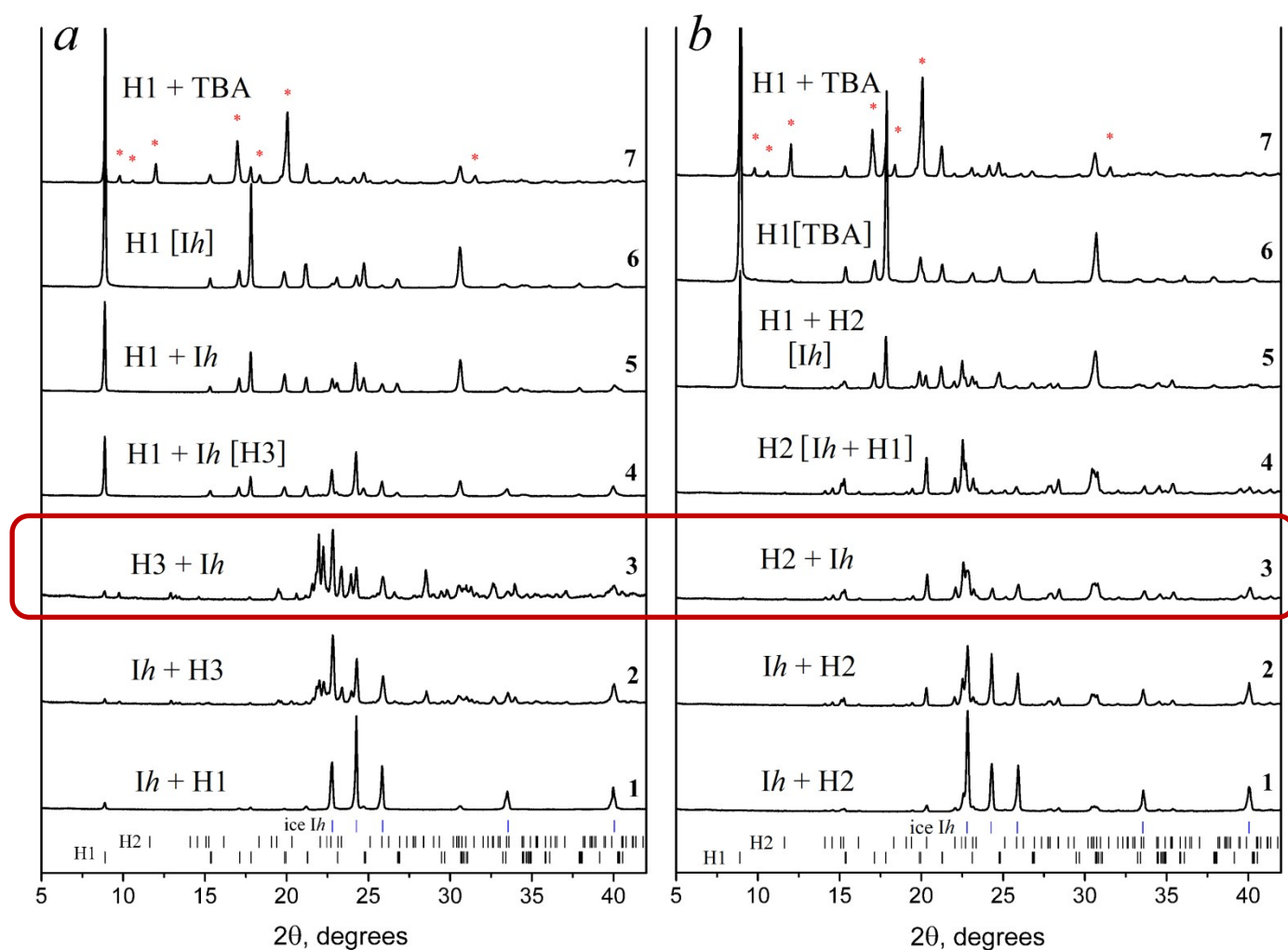


**Figure S23.** Comparison of PXRD patterns of frozen (*a* – protocol II*a*) and subsequently annealed (*b* – protocol II*b*) TBA – water solutions recorded at  $-100^{\circ}\text{C}$ . The positions of reflections of the TBA hydrates (H1 and H2) and ice *Ih* are shown as ticks at the bottom. The positions of reflections of the H3 are neglected for clarity. \* – the strongest reflections of the TBA. 1, 2, 3, 4, 5, 6, 7 correspond to 10, 20, 29.8 (H3), 37 (H2), 55, 70 (H1) and 85 wt % of TBA, respectively. The admixture phases (a few weak reflections on PXRD patterns) are shown in brackets.

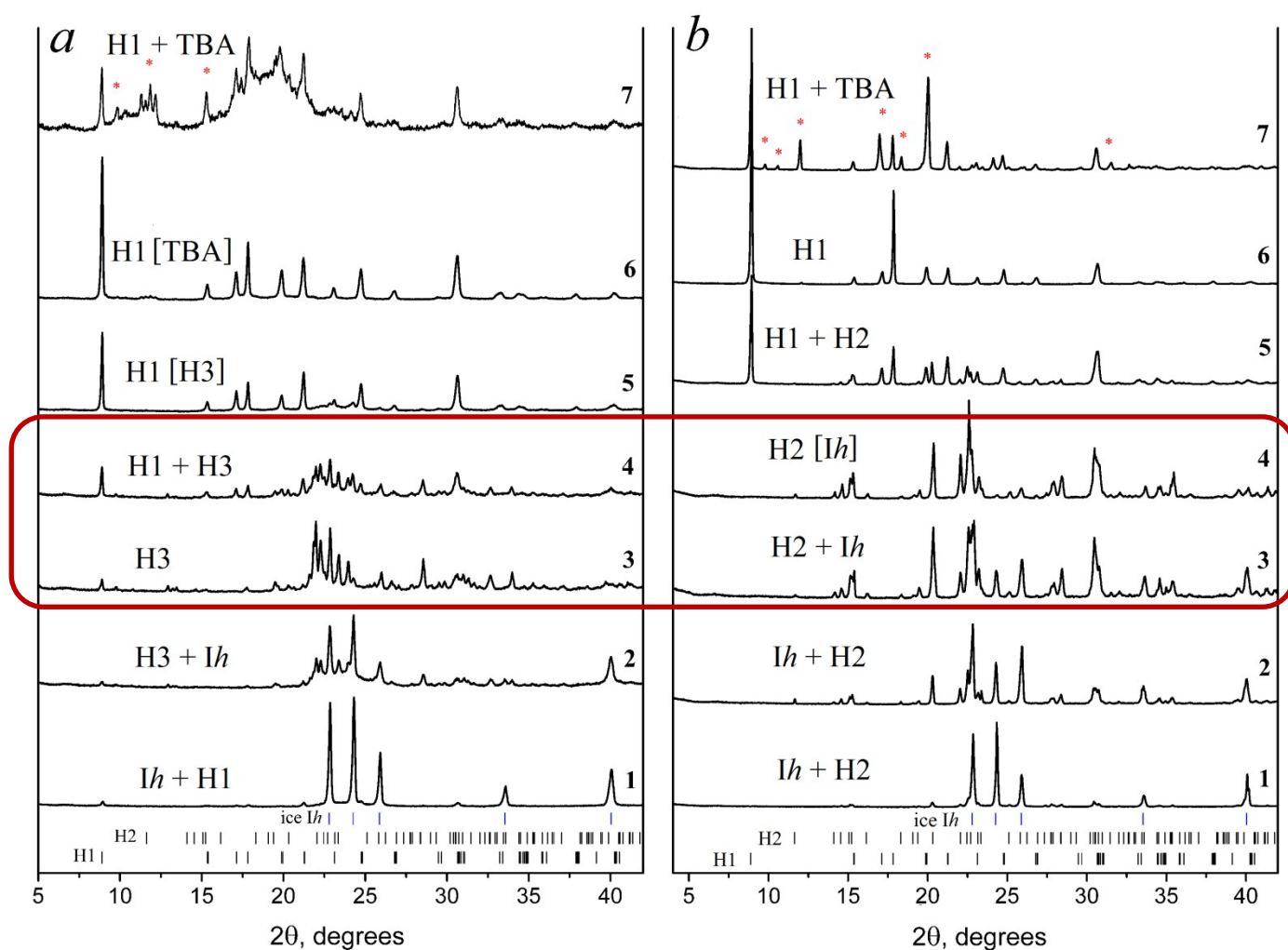


**Figure S24.** Comparison of PXRD patterns of frozen (*a* – protocol III*a*) and subsequently annealed (*b* – protocol III*b*) TBA – water solutions recorded at  $-100^{\circ}\text{C}$ . The positions of reflections of the TBA hydrates (H1 and H2) and ice *Ih* are shown as ticks at the bottom. The positions of reflections of the H3 are neglected for clarity. \* – the strongest reflections of the TBA. 1, 2, 3, 4, 5, 6, 7 – correspond to 10, 20, 29.8 (H3), 37 (H2), 55, 70 (H1) and 85 wt % of TBA, respectively. The admixture phases (a few weak reflections on PXRD patterns) are shown in brackets.



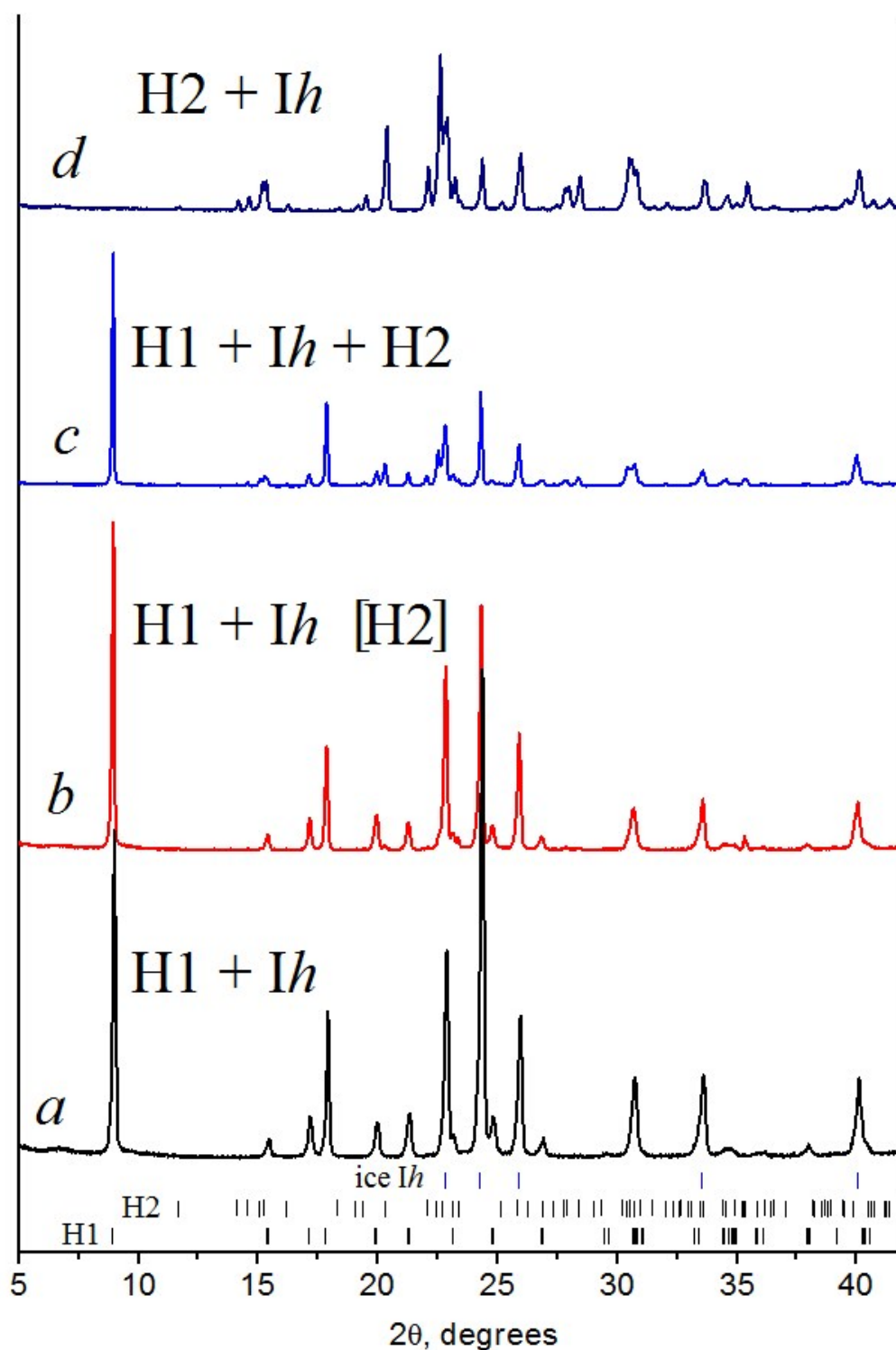


**Figure S25.** Comparison of PXRD patterns of frozen (*a* – protocol Ia) and subsequently annealed (*b*, *c*, *d* – protocol Ib) TBA–water solutions (29.8 wt % of TBA, H3 composition) at different duration of annealing stage (general view) recorded at -100°C. *b* – 12 hours, *c* – 1 month, *d* – 3 months. The admixture phases (a few weak reflections on PXRD patterns) are shown in brackets.

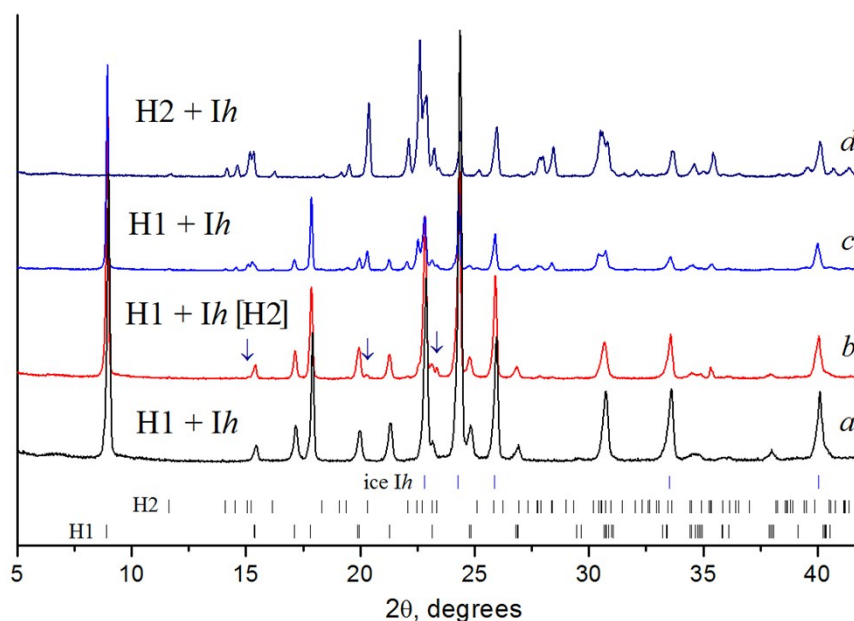


**Figure S26.** Comparison of PXRD patterns of frozen (*a* – protocol Ia) and subsequently annealed (*b*, *c*, *d* – protocol Ib) TBA–water solutions (29.8 wt % of TBA, H3 composition) at different duration of annealing stage recorded at -100°C (enlarged view). *b* – 12 hours, *c* – 1 month, *d* – 3 months. The appearance of reflections of the H2 pointed by navy arrows on *b*. The admixture phases (a few weak reflections on PXRD patterns) are shown in brackets.

**Table S1.** Phases formed from the solutions with the TBA content corresponding to H3 hydrate composition (29.8 wt % of TBA) and calculated weight fraction of TBA hydrates and ice Ih depending on freezing protocol.

Freezing protocol	Crystalline phases	Calculated weight fractions of TBA hydrates and ice Ih
Ia	H1 + Ih	H1 (70 wt % of TBA): 43.3 wt %; Ih: 56.7 wt %
IIIa	H3	H3 (29.8 wt % of TBA): 100 wt %
IIIb/ IIIb_vial	H2 + Ih	H2 (37 wt % of TBA): 78.7 wt %; Ih: 21.3 wt %

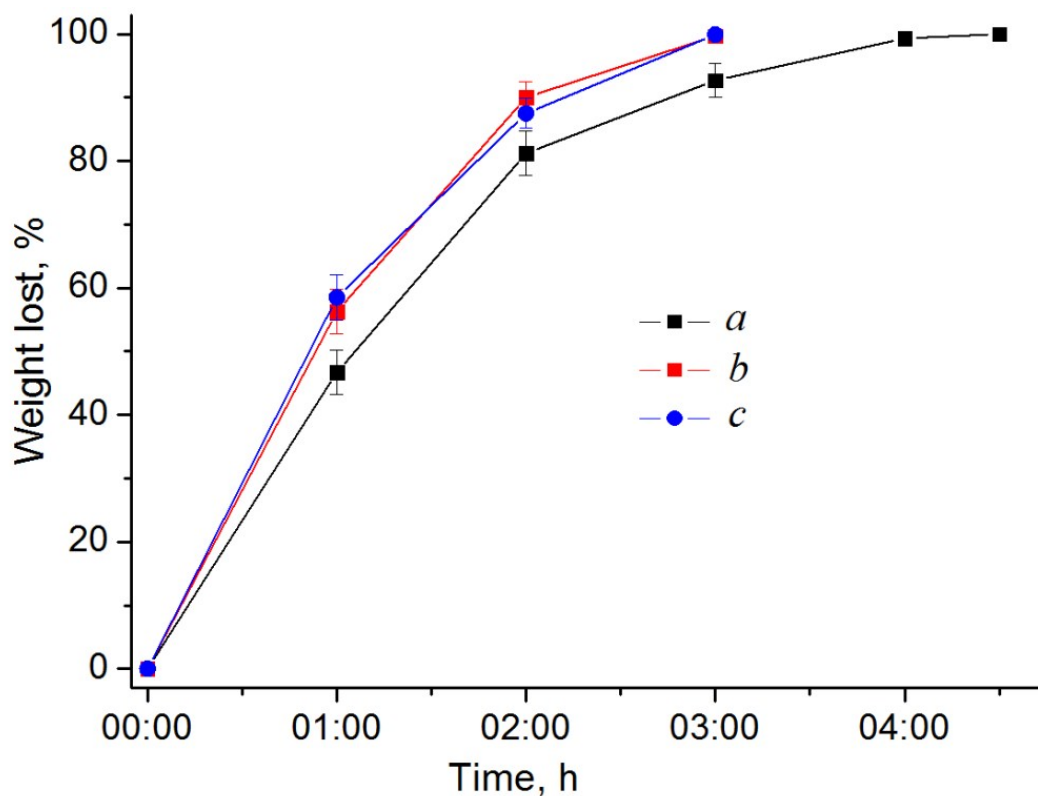


**Figure S27.** Weight loss vs. time for 15 ml glass tubing vials filled with  $2.000 \pm 0.005$  g of TBA – water solution (29.8 wt % of TBA, H3 composition). Shelf temperature was  $-10^{\circ}\text{C}$ , chamber pressure equaled to 100 mTorr. *a* – freezing protocol Ia, solid phases at the beginning of experiment: H1+Ih; *b* – freezing protocol IIIb\_vial, solid phases at the beginning of experiment: H2+Ih; *c* – freezing protocol IIIa\_vial, solid phase at the beginning of experiment: H3.

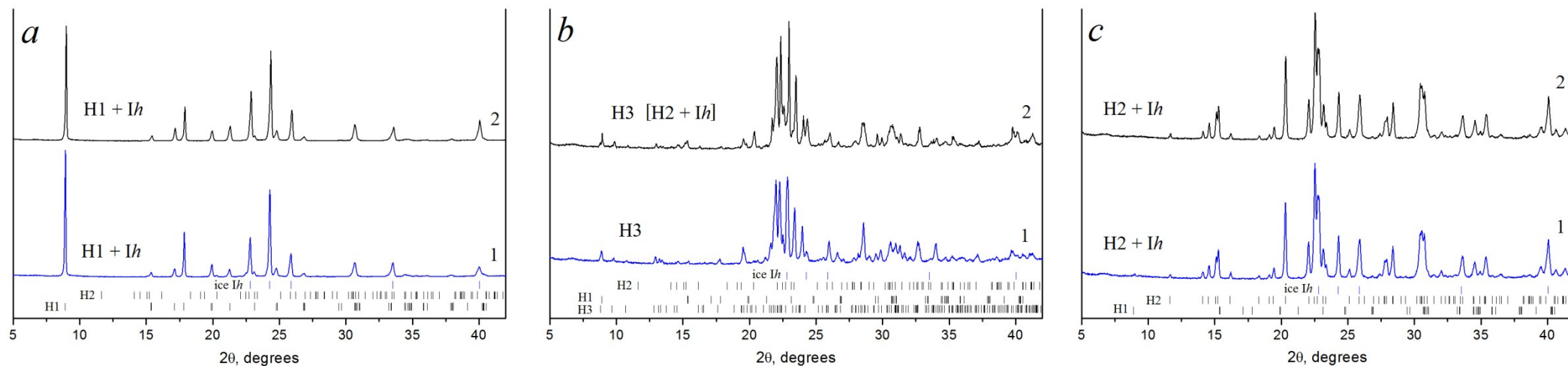


**Figure 28** Results of experiment aimed to determine the sublimation behavior of TBA hydrates in 15 ml glass tubing vials filled with  $2.000 \pm 0.005$  g of TBA – water solution (29.8 wt % of TBA, H3 composition). Shelf temperature was  $-10^\circ\text{C}$ , chamber pressure equaled to 100 mTorr. Comparison of PXRD patterns of the samples (*a*: protocol Ia; *b*: protocol IIIa\_vial; *c*: protocol IIIb\_vial) at different stage of freeze-drying recorded at  $-100^\circ\text{C}$  (1: starting samples (before placed on drying shelf); 2 – after 50 % weight loss). The admixture phases (a few weak reflections on PXRD patterns) are shown in brackets.

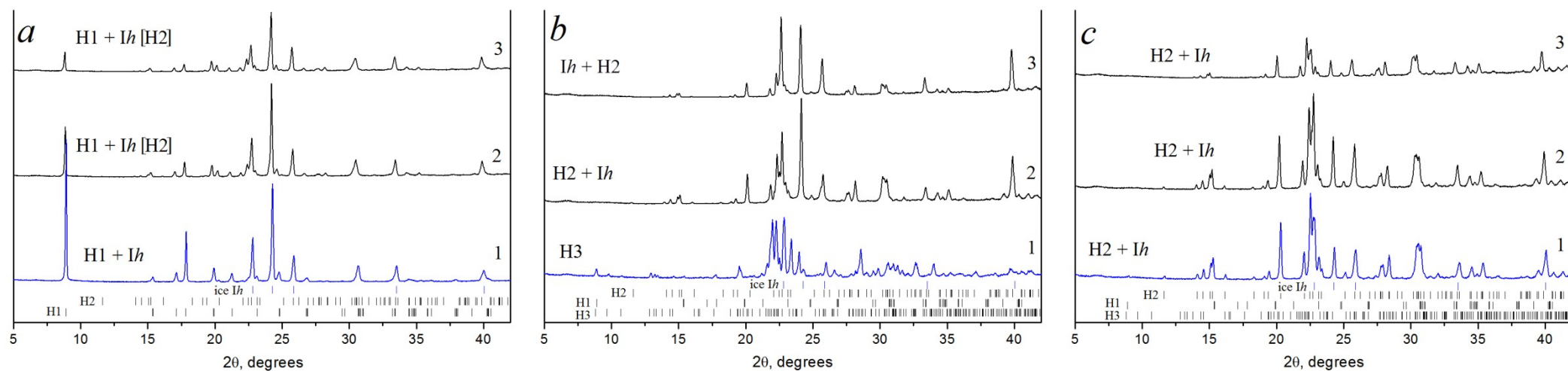


**Figure S29.** Results of experiment aimed to determine the sublimation behavior of TBA hydrates *in situ* in an Anton Paar TTK 450 low-temperature chamber. Comparison of PXR D patterns of samples (29.8 wt % of TBA, H3 composition; *a*: protocol Ia; *b*: protocol IIIa\_vial; *c*: protocol IIIb\_vial) at different stage of freeze-drying (1: starting samples at  $-100^{\circ}\text{C}$ /ambient pressure; 2 and 3: after 10 and 20 minutes at  $-10^{\circ}\text{C}$ /100 mTorr, respectively). The admixture phase (a few weak reflections on PXR D patterns) is shown in brackets.

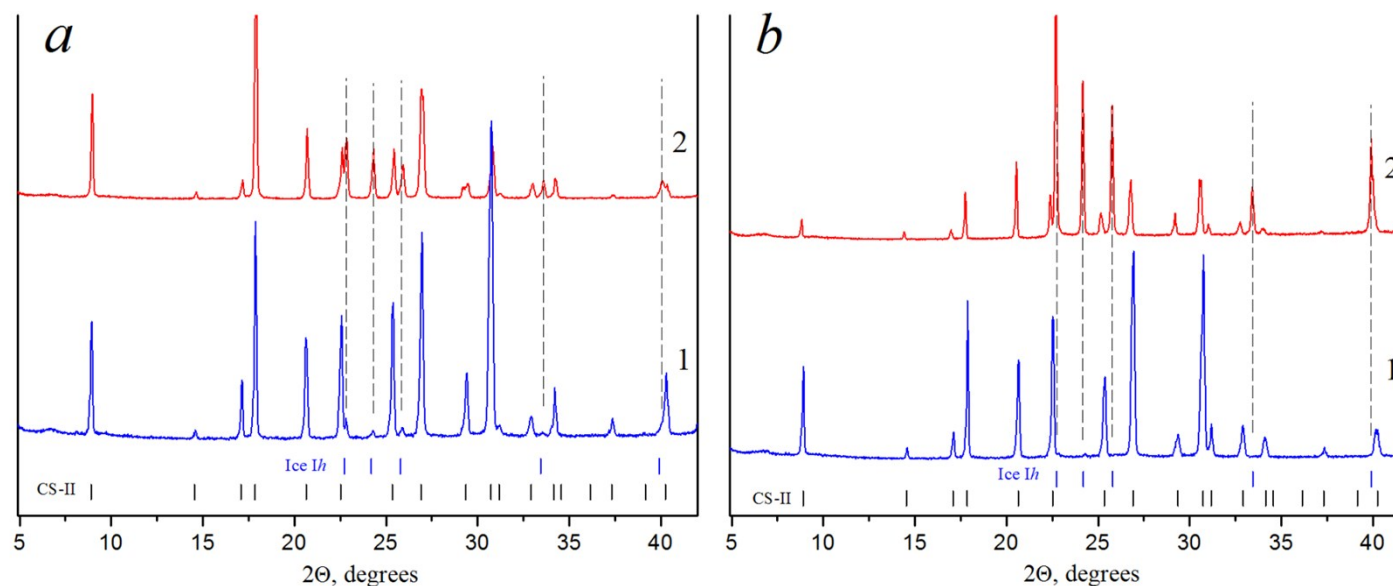


**Figure S30.** Results of experiment aimed to determine the sublimation behavior of THF hydrate in 15 ml glass tubing vials filled with  $2.000 \pm 0.005$  g of THF – water solution (19.1 wt % of THF, THF hydrate composition) (a) *in situ* in an Anton Paar TTK 450 low-temperature chamber (b). Comparison of PXRD patterns of samples at different stage of freeze-drying (a: 1: starting samples (before placed on drying shelf); 2 – after 50 % weight loss; b: 1: starting samples at  $-100^\circ\text{C}$ /ambient pressure; 2: after 20 minutes at  $-10^\circ\text{C}/100$  mTorr, respectively). The positions of the reflections of the CS-II THF hydrate and ice *Ih* are shown as ticks at the bottom.

**Table S2.** Sublimation end points for 15 ml glass tubing vials filled with  $2.000 \pm 0.005$  g of TBA-water solutions (29.8 wt %, H3 composition). Shelf temperature was  $-25^\circ\text{C}$ , chamber pressure equaled to 100 mTorr (sample temperature lower than  $-40^\circ\text{C}$ ).

Freezing protocol/ solid phases at the beginning of experiment	Primary drying time, h
Ia / H1+Ih	6
IIIa_vial / H3	5
IIIb_vial / H2+Ih	5

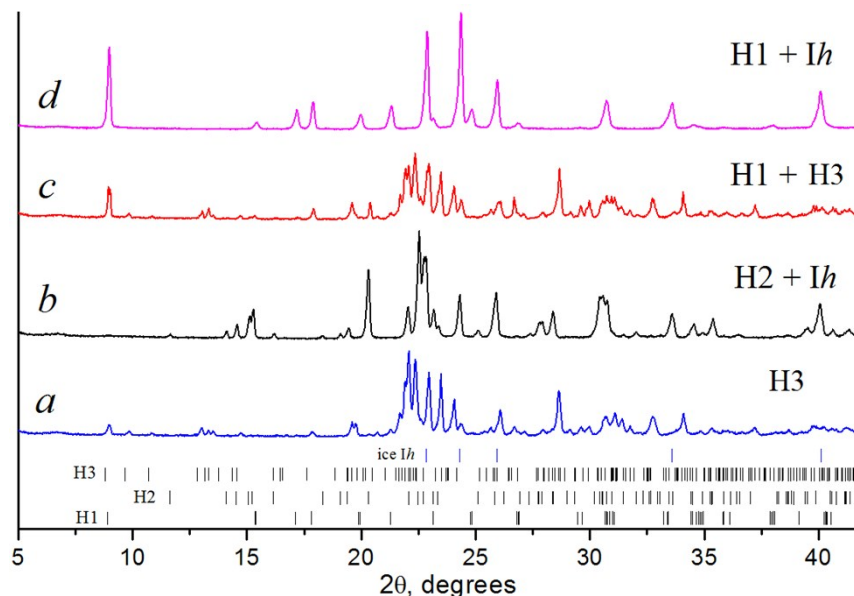


**Figure S31.** PXRD patterns (recorded at  $-100^{\circ}\text{C}$ ) of trehalose solutions in TBA–water co-solvent system (29.8 wt % of TBA, H3 composition), frozen according to different protocols. *a* - freezing protocol IIIa; *b* - freezing protocol IIIb; *c* - freezing protocol IIa; *d* - freezing protocol Ia. The positions of reflections of the TBA hydrates (H1, H2, H3) and ice *Ih* are shown as ticks at the bottom.

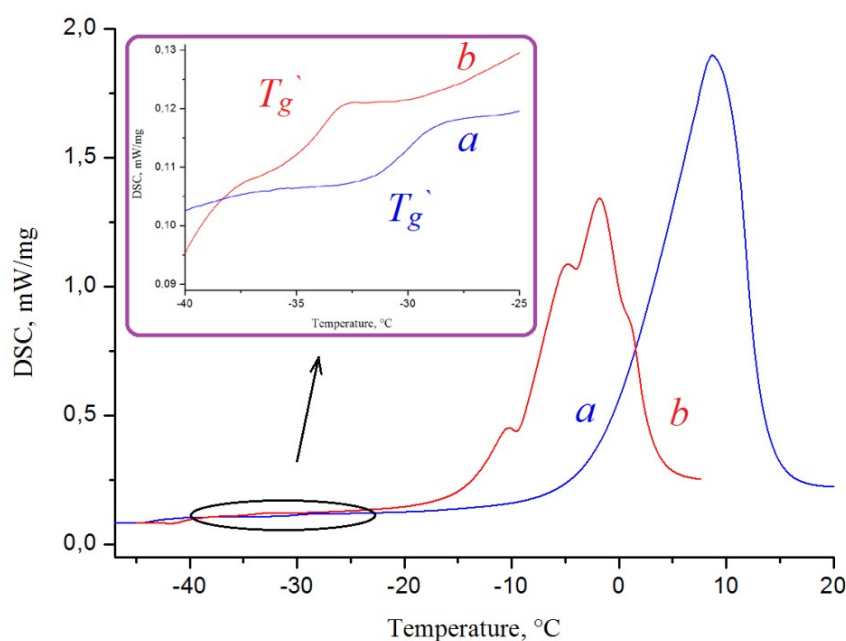


**Figure S32.** DSC curves of frozen trehalose solutions (5 wt % of trehalose) in water (*a*) and TBA–water co-solvent system (29.8 wt % of TBA, H3 composition) (*b*). The change of the slope of the basal lines is zoomed.



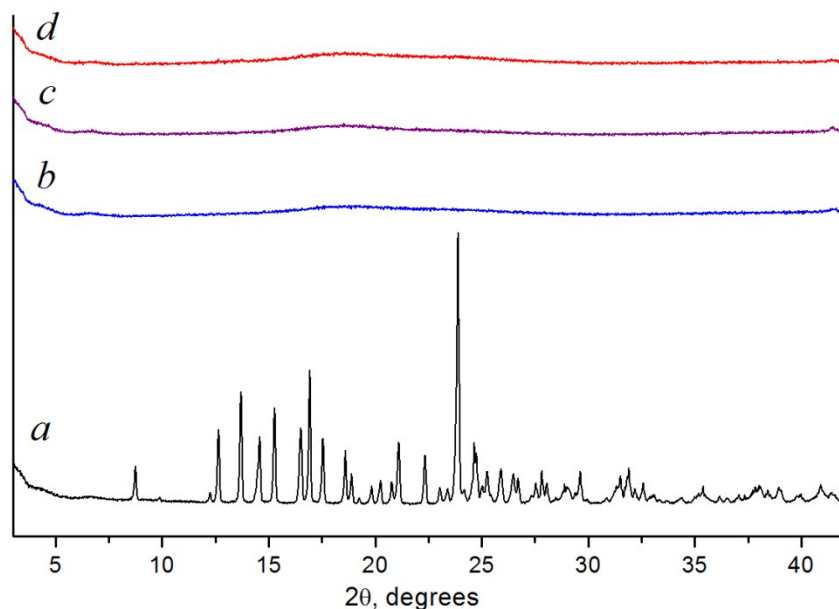


**Figure S33.** PXRD patterns: *a* - starting trehalose dihydrate; *b* - trehalose freeze-dried cake, obtained from aqueous solution (5 wt % of trehalose), freezing protocol Ia; *c* - trehalose freeze-dried cake, obtained from trehalose solution (5 wt % of trehalose) in TBA–water (29.8 wt % of TBA), freezing protocol Ia; *d* - trehalose freeze-dried cake, obtained from trehalose solution (5 wt % of trehalose) in TBA–water (29.8 wt % of TBA), freezing protocol IIIb\_vial.

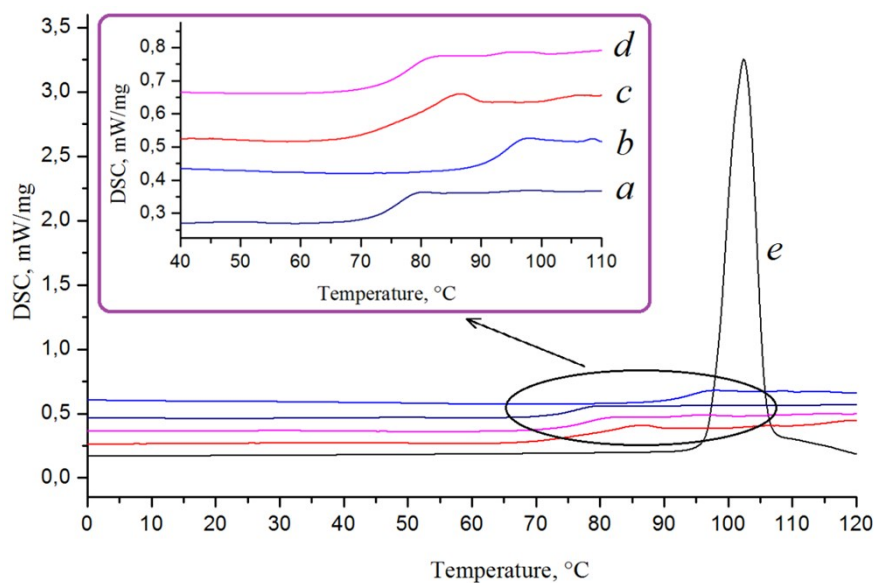


**Figure S34.** DSC curves obtained on heating (6 K/min) of trehalose freeze-dried cakes, prepared from trehalose solutions (5 wt % of trehalose) according to different freezing protocols (*a* - *d*) and starting trehalose dihydrate (*e*). *a* - trehalose freeze-dried cake, obtained from aqueous solution, freezing protocol Ia; *b* - trehalose freeze-dried cake, obtained from aqueous solution, freezing protocol IIIa; *c* - trehalose freeze-dried cake, obtained from trehalose solution in TBA–water (29.8 wt % of TBA), freezing protocol Ia; *d* - trehalose freeze-dried cake, obtained from trehalose solution in TBA – water (29.8 wt % of TBA), freezing protocol IIIa; *e* - trehalose freeze-dried cake, obtained from aqueous solution.

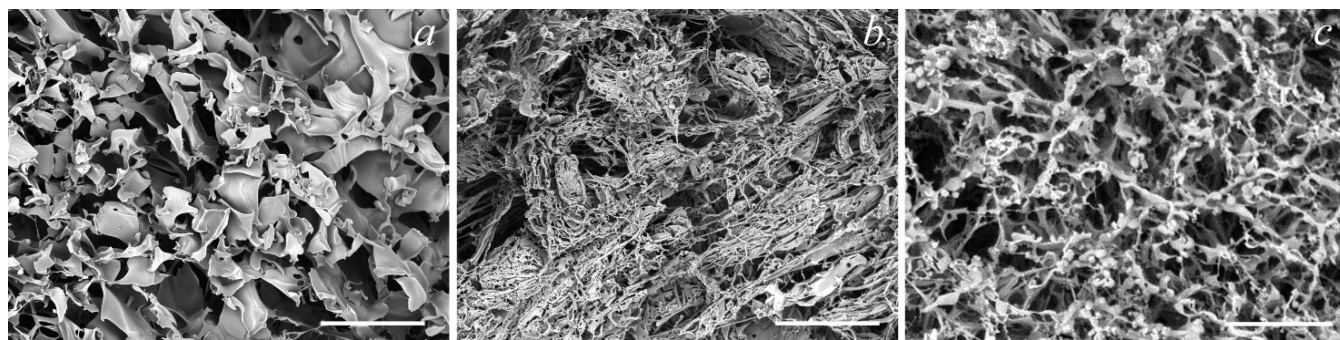


**Figure S35.** Internal structure of the trehalose freeze-dried cakes, prepared from 5 wt % of trehalose solutions according to different freezing protocols. *a* – aqueous solution, freezing protocol Ia, solid phase at the beginning of the experiment: *Ih*; *b* – TBA – water solution (29.8 wt % of TBA), freezing protocol Ia, solid phases at the beginning of experiment: *H1+Ih*; *c* – TBA – water solution (29.8 wt % of TBA), freezing protocol III*b\_vial*, solid phases at the beginning of experiment: *H2+Ih*.

## REFERENCES

- (1) J.-C. Rosso and L. Carbonnel. Le système eau-butanol tertiaire. C. R. Acad. Sci. Paris, Ser. C **1968**, 267, 4.
- (2) J.B. Ott, J.R. Goates and B.A. Waite. (Solid + Liquid) Phase-Equilibria and Solid-Hydrate Formation in Water + Methyl, + Ethyl, + Isopropyl, and + Tertiary Butyl Alcohols. J. Chem. Thermodyn. **1979**, 11(8), 739-746.
- (3) D. Mootz and D. Staben. The Hydrates of Tert-Butanol - Crystal-Structure of  $\text{Me}_3\text{COH}\cdot 2\text{H}_2\text{O}$  and  $\text{Me}_3\text{COH}\cdot 7\text{H}_2\text{O}$ . Z. Naturforsch. **1993**, 48B, 1325-1330.
- (4) M. Woznyj and H.D. Ludemann. The Pressure of Dependence of the Phase-Diagram T-Butanol Water. Z. Naturforsch. **1985**, 40A, 693-698.
- (5) K. Kasraian and P.P. Deluca. Thermal-Analysis of the Tertiary Butyl Alcohol-Water System and Its Implications on Freeze-Drying. Pharm. Res. **1995**, 12, 484-490.
- (6) L. Dobrzycki. Towards Clathrates. 2. The Frozen States of Hydration of tert-Butanol. Z. Krist.-Cryst. Mater. **2018**, 233(1), 41-49.
- (7) S. Vessot and J. Andrieu. A Review on Freeze Drying of Drugs with tert - Butanol (TBA) + Water Systems: Characteristics, Advantages, Drawbacks. Dry. Technol. **2012**, 30, 377-385.
- (8) A.G. Ogienko, V.A. Drebuschak, E.G. Bogdanova, A.S. Yunoshev, A.A. Ogienko, E.V. Boldyreva and A.Yu. Manakov. Thermodynamic aspects of freeze-drying. A case study of an "organic solvent-water" system. J. Therm. Anal. Calorim. **2017**, 127, 1593-1604.
- (9) A.G. Ogienko, E.G. Bogdanova, A.S. Stoporev, A.A. Ogienko, M.P. Shinkorenko, A.S. Yunoshev and A.Yu. Manakov. Preparation of fine powders by clathrate-forming freeze-drying: a case study of ammonium nitrate. Mendeleev Commun. **2018**, 28, 211-213.
- (10) B.S. Chang and N.L. Fischer. Development of an Efficient Single-Step Freeze-Drying Cycle for Protein Formulations. Pharm. Res. **1995**, 12(6), 831-837.
- (11) L.M. Her and S.L. Nail. Measurement of Glass-Transition Temperatures of Freeze-Concentrated Solutes by Differential Scanning Calorimetry. Pharm. Res. **1994**, 11(1), 54-59.
- (12) X.C. Tang and M.J. Pikal. Design of freeze-drying processes for pharmaceuticals: Practical advice. Pharm. Res. **2004**, 21, 191-200.